



# Frequency domain water table fluctuations reveal recharge in fractured aquifers depends on both intense and seasonal rainfall and unsaturated zone thickness

Luca Guillaumot<sup>1</sup>, Laurent Longuevergne<sup>1</sup>, Jean Marçais<sup>2</sup>, Nicolas Lavenant<sup>1</sup>, and Olivier Bour<sup>1</sup>

<sup>1</sup>Univ Rennes, CNRS, Geosciences Rennes - UMR 6118, F-35000 Rennes, France

<sup>2</sup>INRAE, UR Riverly, F-69625 Villeurbanne, France

**Correspondence:** Luca Guillaumot (guillaumot@iiasa.ac.at)

**Abstract.** Groundwater recharge is difficult to estimate, especially in fractured aquifers, because of the spatial variability of the soil properties and because of the lack of data at basin scale. A relevant method, known as the WTF method, consists in inferring recharge directly from the water table fluctuations (WTF) observed in boreholes. However, the WTF method neglects the impact of lateral groundwater redistribution in the aquifer, i.e. assumes that all the WTF are attributable to recharge. In this study, we developed the WTF approach in the frequency domain to better consider groundwater lateral flow, which quickly redistributes the impulse of recharge and mitigates the link between WTF and recharge. First, we calibrated a 1D analytical groundwater model to estimate hydrodynamic parameters at each borehole. These parameters were defined from the WTF recorded for several years, independently of prescribed potential recharge. Second, calibrated models are reversed analytically in the frequency domain to estimate recharge fluctuations (RF) at weekly to monthly scales from the observed WTF. Models were tested on two twin sites with similar climate, fractured aquifer, and land use but different hydrogeologic settings: one has been operated as a pumping site for the last 25 years (Ploemeur, France) while the second has not been perturbed by pumping (Guidel). Results confirm the important role of rainfall temporal distribution to generate recharge. While all rainfall contribute to recharge, the ratio of recharge to rainfall minus potential evapotranspiration is frequency dependent, varying between 20 – 30 % at periods < 10days, 30 – 50 % at monthly scale, and reaching 75 % at seasonal time scales. We further show that the unsaturated zone thickness controls the intensity and timing of RF. Overall, this approach contributes to better assess recharge and enable to improve the representation of groundwater systems within hydrological models. In spite of the heterogeneous nature of aquifers, parameters controlling WTF can be inferred from WTF time series.

## 1 Introduction

Increasing anthropogenic and climate pressures on water resources calls for a better understanding of the way water is transiently stored and flows in the subsurface (Gleeson et al., 2012; Wada et al., 2016). Groundwater (GW), as the world largest



accessible freshwater storage, is crucial for water management (Taylor et al., 2013; Alley et al., 2002). GW indeed sustains river (Schaller and Fan, 2009) and ecosystems (Maxwell and Condon, 2016; Fan, 2015), supports food security (Scanlon et al., 2012; Dalin et al., 2017) and secures drinking water (MacDonald and Calow, 2009). Therefore, under global changes, climate variability is expected to intensify the strategic importance of GW to human adaptation (Gerten et al., 2013).

Recharge, as the main water inflow feeding GW, is critical for the proper management of GW systems. GW recharge is defined as the water percolating from the last unsaturated horizon down to the water table and is therefore broadly inaccessible to direct observations (Scanlon et al., 2006; Healy and Cook, 2002). Although it can be measured by a lysimeter or different tracing methods (Scanlon et al., 2002), such methods are subject to spatial variability and difficult to upscale. Recharge is indeed spatially heterogeneous and controlled by multiple factors such as vegetation (Riedel and Weber, 2020; Perkins et al., 2014), soil properties (Kollet, 2009; Sililo and Tellam, 2000; Mohan et al., 2017) and hydrogeological conditions (Kollet and Maxwell, 2008; Fan et al., 2019; Appels et al., 2015).

Modeling the recharge is therefore a relevant method to estimate it. Several recharge models have been developed (Healy, 2010; Simunek et al., 2005), ranging from a fraction of annual precipitation to more complex land surface models resolving energy and water budgets from local to regional scale (Morton, 1983; Thornthwaite, 1948; Wada et al., 2010; Döll and Fiedler, 2008; Mohan et al., 2017; Hartmann et al., 2017). All of these studies assess the GW recharge "from above" (ie. from the surface towards the aquifer). Such approach is hampered by uncertainties in the estimation of surface fluxes (rainfall, evapotranspiration, runoff) (Long et al., 2014; Riedel and Weber, 2020), soil model structural errors, and hydrodynamic properties variabilities and uncertainties (Hartmann et al., 2017; Lee et al., 2006; Nicolas et al., 2019). Moreover, this approach, where modeled soil thickness is limited to a few meter, does not consider the actual water table depth (Clark et al., 2017). We argue these estimates provide only "potential GW recharge" (Figure 1) because of potential storage changes and lateral flow in the deep unsaturated zone (Besbes and Marsily, 1984; Vergnes et al., 2014; Hector et al., 2018).

At the opposite, GW recharge can also be estimated "from below". GW levels in boreholes are indeed the most direct observation to characterize aquifers behavior. The water table fluctuation method (WTF) has thus been used to provide vertical recharge estimates from GW level variations (Healy and Cook, 2002; Crosbie et al., 2005; Cuthbert, 2010; Maréchal et al., 2006; Cuthbert et al., 2016, 2019a; Labrecque et al., 2020). However, GW level variations are also influenced by GW lateral flows, themselves depending on GW boundary conditions, making difficult the estimation of the recharge from below. Main uncertainties arise from the limited knowledge on hydrodynamic parameters, such as specific yield, and the limitation of one observation point to infer flow characteristics in heterogeneous aquifers. Several authors therefore proposed to apply a frequency analysis between long-term data of recharge and GW levels assuming an equivalent homogeneous aquifer (Gelhar, 1974). In this case, time lags and amplitudes of aquifer response to periodic recharge can be described by a linear transfer function (Jimenez-Martinez et al., 2013; Townley, 1995). Based on this theoretical framework, Dickinson (2004) inverted the method to infer time varying recharge linked to climate variability from GW levels. However, this method focuses on long-term periodic cycles.

While strong attention has been put on mean annual recharge estimations, characterizing recharge fluctuations over time (RF), at short to long time scales, remain critical and has been less investigated. This has been highlighted as one of the 23



unsolved problems in hydrology (Blöschl et al., 2019). Recharge is highly variable throughout the year, showing a pronounced seasonality (Jasechko et al., 2014; Gabrielli and McDonnell, 2018) with potential high sensitivity to intense rainfall events (Taylor et al., 2012; Owor et al., 2009; Mileham et al., 2009). RF are also modulated by water table depth, human actions such as pumping (Bredehoeft, 2002) or return flow from irrigation (Taylor et al., 2013; Guihéneuf et al., 2014; Le Coz et al., 2013). Several authors highlighted that changes in recharge impact groundwater flow. For example, irrigation and GW abstraction impact recharge and discharge variability in space and time (Cao et al., 2016; Lee et al., 2006; Shamsudduha et al., 2011; Johansen et al., 2011). Another example is that topographic control on GW flow depends on recharge (Bresciani et al., 2016; Marçais et al., 2017). Recently, several works also documented that modifications to surface or subsurface characteristics (soil properties, vegetation, ...) would affect the hydrological response - including groundwater - at annual to interannual time scales (Ajami et al., 2017; Troch et al., 2009; Fan, 2015; Condon and Maxwell, 2017; Favreau et al., 2009).

In this study, we propose to quantify the RF by developing a novel method able to quantify the GW recharge « from below ». The main objectives of this work are thus threefold: (1) deciphering the respective impact of GW lateral flow and recharge on GW level fluctuations in heterogeneous aquifers; (2) estimating RF over a 20-year period (3) studying how rainfall distribution and unsaturated zone thickness controls GW recharge. To do that, we develop the WTF method in the frequency domain to deconvolute in GW levels observations, GW lateral flows from RF (section 1). While GW systems are heterogeneous in nature, we propose to represent them by an equivalent homogeneous 1D Dupuit model (Fig. 1). We apply this method on two fractured crystalline aquifers, one heavily pumped and one in natural context. We also test the consistency of this newly developed method among the different observations wells of the two sites. For each well, we first estimate hydrodynamic parameters before inverting analytically the model to propose RF estimates. Although simple, the GW model (section 2) can adapt to different boundary conditions as illustrated by the two application sites. Associated GW level observations and prescribed potential recharge rates are presented on section 3. Once the model reproduces GW level fluctuations (section 4), RF can be inverted analytically (section 5). Finally, RF between the two sites are compared and main results are discussed (section 6).

## 2 Modeling approach: from water table to water transfer within the unsaturated zone

### 2.1 Main steps

The method developed in this study relies on several steps as illustrated by Figure 1. The initial step consists of providing a first estimate of potential groundwater recharge for the study area. These data are given at a daily time step. Then, GW analytical model is defined in function of the boundary conditions for each observation well of the study site. The next step consists in calibrating model parameters by comparing simulated WTF to WTF observed in boreholes (Step 1 on Figure 1). The method allows deciphering the respective impact of GW lateral flow and recharge on WTF. To achieve this goal, hydrodynamic parameters are calibrated by prescribing different sets of potential RF. Then, the GW model is reversed analytically (Step 2 on Figure 1) using calibrated parameters at each borehole in the aim to compute RF from observed WTF. While unsaturated zone thickness is not considered during Step 1 (potential recharge equals recharge), it is expected that Step 2 reveals its importance.

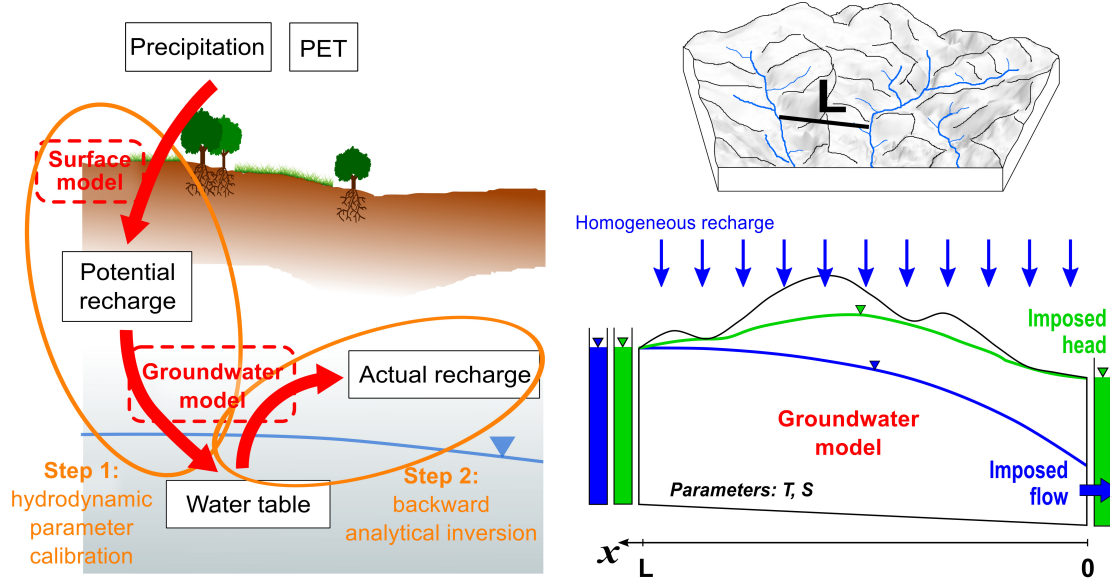


**Figure 1.** On the left: description of the method to estimate recharge from observed water table fluctuations; Step 1 infers groundwater model parameters using potential recharge estimates as input; Step 2 consists in estimating actual recharge from observed water table fluctuations using parameters (obtained from Step 1) in a backward analytical inversion; *PET* refers to potential evapotranspiration. On the right: description of the homogeneous 1D groundwater flow model; recharge rate,  $R(t)$ , is uniformly distributed along model length  $L$ ; model boundary conditions can be constant head or imposed flow rate in order to represent natural (green case) and pumped systems (blue case).

As developed below, we focus on water table and recharge anomalies, here called "fluctuations". These fluctuations are obtained by removing the mean value from input data (potential recharge and pumping rates used during Step 1) over the study period. Consequently, simulated WTF obtained during Step 1 will be compared to observed fluctuations. Finally, RF are obtained from observed WTF (Step 2) and will be compared to potential RF.

In the next sections, we describe (1) the analytical GW flow model deployed to estimate recharge from observed WTF; (2) the soil models used to estimate potential recharge as input to the GW model; (3) the GW parameters calibration strategy and (4) the analytically inverted GW model. Finally, we also present how inverted recharge is analyzed with rainfall at the two study sites.

## 2.2 Defining the 1D flow model for each field site

Considering a homogeneous and confined aquifer, and assuming that the vertical component of the GW flow can be neglected (Dupuit assumption), the GW flow equation can be described by a diffusion equation (Eq. 1) (De Marsily, 1986):

$$T \frac{\partial^2 h(x,t)}{\partial x^2} = S \frac{\partial h(x,t)}{\partial t} - R(t) \quad (1)$$



100 where  $h(x, t)$  are hydraulic head variations [ $L$ ];  $R(t)$  the uniformly distributed recharge rate from the surface [ $L.T^{-1}$ ];  $T$  the aquifer transmissivity [ $L^2/T$ ] and  $S$  the storage coefficient of the aquifer [-]. This formulation is also valid in unconfined aquifers if head variations are small compared to the aquifer thickness. In this case,  $S$  is equivalent to specific yield. The system is defined by a domain comprised between  $x = 0$  and  $x = L$  (Fig. 1).

Solving equation 1 requires two boundary conditions imposed at  $x = 0$  and  $x = L$ . In what follows, we consider an imposed head ( $h_L$ ) at  $x = L$  and either an imposed flux ( $Q_{pump}(t)$ ) or an imposed head ( $h_0$ ) at  $x = 0$  depending on the site considered (respectively the pumping site and the "natural" case). These boundary conditions have been chosen to best represent actual aquifer configurations. Equation 1 with the associated boundary conditions can be solved analytically in the frequency domain (Townley, 1995; Carslaw and Jaeger, 1959) and lead to equations 2 and 3 describing WTF ( $h(x_r, t)$ ). The full derivation of these equations is provided in Appendix A.

$$h(x_r, t) = \sum Re\{e^{i\omega t} \left[ \frac{\bar{R}}{i\omega S} \left( 1 - \frac{\cosh(x_r \sqrt{i\omega t_c})}{\cosh(\sqrt{i\omega t_c})} \right) + \frac{\bar{Q}}{W} \frac{L}{T \sqrt{i\omega t_c}} \frac{\sinh(\sqrt{i\omega t_c}(x_r - 1))}{\cosh(\sqrt{i\omega t_c})} \right]\} \text{ (pumping site)} \quad (2)$$

$$h(x_r, t) = \sum Re\{e^{i\omega t} \left[ \frac{\bar{R}}{i\omega S} \left( 1 + \frac{\sinh(\sqrt{i\omega t_c}(x_r - 1)) - \sinh(x_r \sqrt{i\omega t_c})}{\sinh(\sqrt{i\omega t_c})} \right) \right]\} \text{ (natural site)} \quad (3)$$

110 with  $D = \frac{T}{S}$ ,  $X = \sqrt{\frac{D}{i\omega}}$ ,  $x_r = \frac{x}{L}$  and  $t_c = \frac{L^2}{D}$

Equations 2 and 3 highlight the importance of characteristic time ( $t_c$ ) (Domenico and Schwartz, 1998) describing how a pressure pulse is propagated along the distance  $L$ . Note that the pumping case requires input for model width  $W$  to define a volume per unit of time (see Figure A.1 and Appendix A.2). While GW pumping are actually localized in boreholes, boundary conditions should be applied along the width  $W$  of the 1D model. The weak impact of parameter  $W$  in estimating hydrodynamic parameters and recharge is assessed separately in the Supporting Information (SI). In addition, the approach was also tested in radial coordinates to compare the impact of model geometry in the pumping case (SI). Several analytical solutions corresponding to different hydrogeological configurations are also provided in the attachment to this study. The analytical model is evaluated in Appendix B.1 by comparing WTF obtained from equation 3 to WTF obtained from a numerical model with similar geometry and parameters.

120 Equations 2 and 3 describe WTF as a function combining the Fourier transform of the recharge and the pumping ( $\bar{R}$  and  $\bar{Q}$ ) modulated by the transient events frequency ( $\omega$ ) with respect to  $t_c$  so that high frequencies are dampened, and a geometric function defined by the monitoring well relative position ( $x_r$ ) inside the domain, here the distance to the pumping wells. These analytical solutions do not depend on the constant head imposed at  $x = L$ , and at  $x = 0$  for the natural case. Therefore, WTF are not impacted by the mean hydraulic gradient which constitutes a major advantage of our method by reducing the number of parameters and uncertainty on the input lateral flow at  $x = L$  (see Appendix C dealing with the steady part of equation 1).



### 2.3 Estimating potential recharge "from above"

The GW model described previously is driven by GW recharge  $R(t)$ . In order to assess GW model sensitivity to prescribed recharge estimates, we tested three different classical soil models computing potential recharge "from above" (from the surface towards the aquifer as described in figure 1). These three potential recharge data differ in term of mean value and time-  
130 dependent fluctuations. Soil models use daily climate data to infer daily potential recharge defined as percolation below the root zone. We consider that potential recharge is instantaneously input to the GW system as actual recharge, thereby neglecting unsaturated zone processes between the modeled soil layer and the actual water table depth. To focus on the temporal fluctuations and avoid the issues related to the steady part (see Appendix C), we subtract the mean value from the modeled potential recharge data before providing them to the GW analytical model.

135 The first - and simplest soil model, called "Thorntwaite" is based on the representation of the unsaturated zone as a simple reservoir accumulating rainwater and satisfying potential evapotranspiration (calculated using the Thorntwaite method) while water is available. When the reservoir is full, excess water recharges GW (Thorntwaite, 1948). Such a model neglects surface runoff. In Brittany, surface runoff is expected to be relatively low for most of the year due to moderate rain intensities, lack of high reliefs and steep slopes and vegetation that favors infiltration. Based on previous studies on the Ploemeur site (Jimenez-  
140 Martinez et al., 2013), we consider a soil storage reserve of 166 mm based on a local soil characterization.

The second soil model is derived from the GR4J hydrological model (Perrin et al., 2003). Potential recharge estimates are based on the so called production store and defined as the sum of downward fluxes out of the production store (see <https://webgr.irstea.fr/modeles/journalier-gr4j-2/>). In this model, evapotranspiration and other water fluxes depend on the amount of water stored in the reservoir in a non-linear but incremental way, providing more diffuse infiltration as compared to  
145 the previous model. After several tests, the capacity of the production store is set to 300 mm in order to provide more recharge with a more diffuse behavior compared to the Thorntwaite model.

The third potential recharge estimate is provided by the SURFEX modeling platform. SURFEX is composed of a spatially distributed land surface model (Interaction between Soil Biosphere and Atmosphere - ISBA) that simulates water and energy fluxes at the interface between atmosphere and surface (soil, vegetation, snow) (Noilhan and Planton, 1989; Masson et al.,  
150 2013). SURFEX is provided on a 8-km grid over France. Potential recharge corresponds to the water drained below the root zone, also called 'deep drainage'.

### 2.4 GW model parameters calibration

The forward model is now fully defined. The first step of our approach consists in defining geometric ( $L$  and  $W$ ) and hydrodynamic ( $T$  and  $S$ ) parameters based on the comparison with measured groundwater levels. In the pumping case,  $W$  was chosen  
155 arbitrarily to be  $W = 1000$  m as a first parameter set exploration showed that this parameter did not influence results as long as  $W > 500$  m (SI).  $W$  does not appear in the analytical solution of the natural case. The location  $x$  of the observation wells also needs to be defined consistently with the 1D framework. In the pumping case,  $x$  is defined as the distance to the pumping wells.



In the natural case,  $x$  is defined as the distance to the river (lower boundary condition). Two examples of model alignment are illustrated in Figure 2.

160 In order to explore the informative content of the observed WTF to define geometric and hydrodynamic parameters, our strategy consists in defining equiprobable parameter sets testing sensitivity to imposed recharge rates (section 2.3). Analytical GW models are computationally efficient. Thus, the whole parameter space ( $T$ ,  $S$ ,  $L$ ) has been regularly sampled (in a logarithmic scale for  $T$  and  $S$ ) inside a plausible range defined by values reported in comparable geological settings of Brittany and beyond: transmissivity  $T \in [10^{-4}; 2 \times 10^{-1}] m^2.s^{-1}$  (40 values), storage coefficient  $S \in [10^{-4}; 2 \times 10^{-1}]$  (40 values), length  
 165  $L \in [800; 6000] m$  (53 values). We refer to Le Borgne et al. (2006) and Leray et al. (2014) regarding hydrodynamic properties expected on Ploemeur site. Regarding storage coefficient, a 0.01-0.2 range can be considered to reflect weathered and fissured horizons (see Kovacs (1981), Wright and Burgess (1992) and Singhal and Gupta (2010) for values in shallow weathered zones and Earle (2015) and Hiscock (2009) for granites and schists). For Guidel site, length  $L$  varies between 20 and 2000  $m$  with 100 values. This range is smaller because  $L$  is expected to be smaller in 'natural conditions' compared to pumping conditions  
 170 where water table drawdown tends to extend the system (Fig. 1). In Brittany, the hillslope length is typically 1  $km$  (Lague et al., 2000). In addition, three sets of potential recharge rates have been imposed on the Ploemeur site model. So, a total of 254400 and 160000 simulations were run for each monitoring well for Ploemeur and Guidel sites respectively. This approach allows estimation of the extent to which model parameters can be defined with observed WTF. In order to reduce computing time during model calibration, the model is run at a 7-day time step.

175 Modeled WTF are evaluated against root mean square error ( $RMSE$ ) divided by the standard deviation of observed WTF (called normalized RMSE:  $nRMSE$ ) to favour comparison among the different observation wells:

$$nRMSE = \sqrt{\frac{\sum (h_{obs} - h_{model})^2}{n}} \times \frac{1}{\sigma_{obs}} \quad (4)$$

where  $n$  is the samples number along time and  $\sigma_{obs}$  is the standard deviation of observed data along time.

## 2.5 Backward model

In a last step, GW recharge ( $R(t)$ ) is analytically determined from equation 2 for the pumping case. Indeed, when hydrodynamic  
 180 parameters (section 2.4) and boundary conditions ( $Q(t)$ ) are known, WTF ( $h_{obs}(x, t)$ ) can be reversed analytically (Appendix A.3) in frequency domain in order to infer the Fourier transform of recharge (Eq. 5):

$$\bar{R}(\omega) = \left( i\omega S \bar{h}(x_r, \omega) - \frac{\bar{Q}}{W} \frac{\sqrt{i\omega t_c} \sinh(\sqrt{i\omega t_c}(x_r - 1))}{\cosh(\sqrt{i\omega t_c})} \right) \times \left( 1 - \frac{\cosh(x_r \sqrt{i\omega t_c})}{\cosh(\sqrt{i\omega t_c})} \right)^{-1} \quad (5)$$

$\bar{R}(\omega)$  appears expressed as an equivalent water layer ( $S \cdot \bar{h}$ ) minus the impact of pumping  $\bar{Q}/W/L$  redistributed on the system by a space-time function (sine and cosine hyperbolic functions). Finally, a geometric parameter ( $x_r = x/L$ ) defining monitoring well positions within the system controls recharge amplitude, as a well head variation integrates both vertical and lateral  
 185 recharge. Note that backward models are run at daily time step to benefit from the observed WTF and because backward models are run only with a set of best parameters (section 2.4).



A similar analytical solution is obtained for the case without pumping from equation 3, as described by equation 6.

$$\bar{R}(\omega) = i\omega S \bar{h}(x_r, \omega) \left( 1 + \frac{\sinh(\sqrt{i\omega t_c}(x_r - 1)) - \sinh(x_r \sqrt{i\omega t_c})}{\sinh(\sqrt{i\omega t_c})} \right)^{-1} \quad (6)$$

Then, RF are computed by inverse Fourier transform. RF uncertainties are evaluated by propagating parameter uncertainties. Thus, for both cases, RF can be estimated from WTF taking into account lateral flow and unsaturated zone influence in contrast to classical method computing recharge from above (described in section 2.3).

This new approach has been evaluated with a numerical MODFLOW model (see Appendix B). The evaluation consists of providing daily recharge rates (Thornthwaite model) to a numerical model equivalent to the analytical 1D model used for the Guidel case. The resulting WTF at  $x_r = 0.75$  are then used in equation 6 to estimate RF. Similar RF estimates would lend support for the analytical approach. We found that analytically estimated RF are similar at the 1% level to the reference 'Thornthwaite' RF integrated over 10-day time steps. Thus, the analytical model allows to estimate RF accurately on an ideally designed site (known parameters and simple 1D geometry). This numerical test also brings first insights on the impact of parameters uncertainty on estimated recharge: a factor 2 uncertainty in storativity  $S$  directly corresponds to a factor 2 uncertainty in recharge volumes, considering other parameters are fixed, while uncertainty on characteristic time is less pronounced.

## 2.6 How unsaturated zone transforms precipitation into recharge

Finally, rainfall fluctuations obtained from climate data and RF obtained by inverting the best GW models are analyzed at both sites in time and frequency domains. In order to focus on the transformation of rainfall into recharge, we compute both the coherence and the transfer function (Jimenez-Martinez et al., 2013) between recharge and rainfall minus potential evapotranspiration  $P - PET$  (also expressed as anomalies). The coherence  $C_{XY}(\omega)$  examines the relationship between two signals  $\bar{X}(\omega)$  ( $P - PET$  fluctuations) and  $\bar{Y}(\omega)$  (recharge fluctuations) by computing the frequency-dependent correlation, defined as:

$$C_{XY} = \frac{P_{XY}(\omega)^2}{P_{XX}(\omega)P_{YY}(\omega)} \quad (7)$$

where  $P_{XY}$  is the cross-spectral density between X and Y, and  $P_{XX}$  and  $P_{YY}$  are the autospectral density of x and y respectively. The transfer function  $\bar{H}(\omega)$  describes the amplitude ratio between output and input in the frequency domain as:

$$\bar{Y} = \bar{H} \bar{X} \quad (8)$$

Thus, the transfer function quantifies  $P - PET$  efficiency to recharge GW, ie. a proxy of rainfall efficiency. These functions allow to infer the role of the soil and more generally of the unsaturated zone. As a comparison, we also computed coherence and transfer functions between  $P - PET$  and potential recharge. Here, we used 'mscohere' and 'tfestimate' Matlab functions. Coherence and transfer function are computed by dividing overlapping sections of 280 days, windowed by a Hamming function, and overlapping by 50%.



### 3 Application sites and data

#### 3.1 The Ploemeur and Guidel observatories

Model ability to estimate RF is tested on the Ploemeur-Guidel hydrogeological observatory (<http://hplus.ore.fr/en/ploemeur>), being part of  $H^+$  network (<http://hplus.ore.fr/en/>) and the French Critical Zone network OZCAR (<http://ozcar-ri.org/>) (Gailardet et al., 2018). Neighboring sites (Fig. 2) are set in a similar climatic, geologic and land cover context. The landscape consists of fields and meadows with slight topography (average slope around 3 %). GW is hosted in highly fractured crystalline rocks (Ruelleu et al., 2010; Touchard, 1999; Jimenez-Martinez et al., 2013). Ploemeur site has been pumped since 1991 while Guidel site has not been perturbed by pumping and hosts large GW upflowing zones creating groundwater-dependent ecosystems.

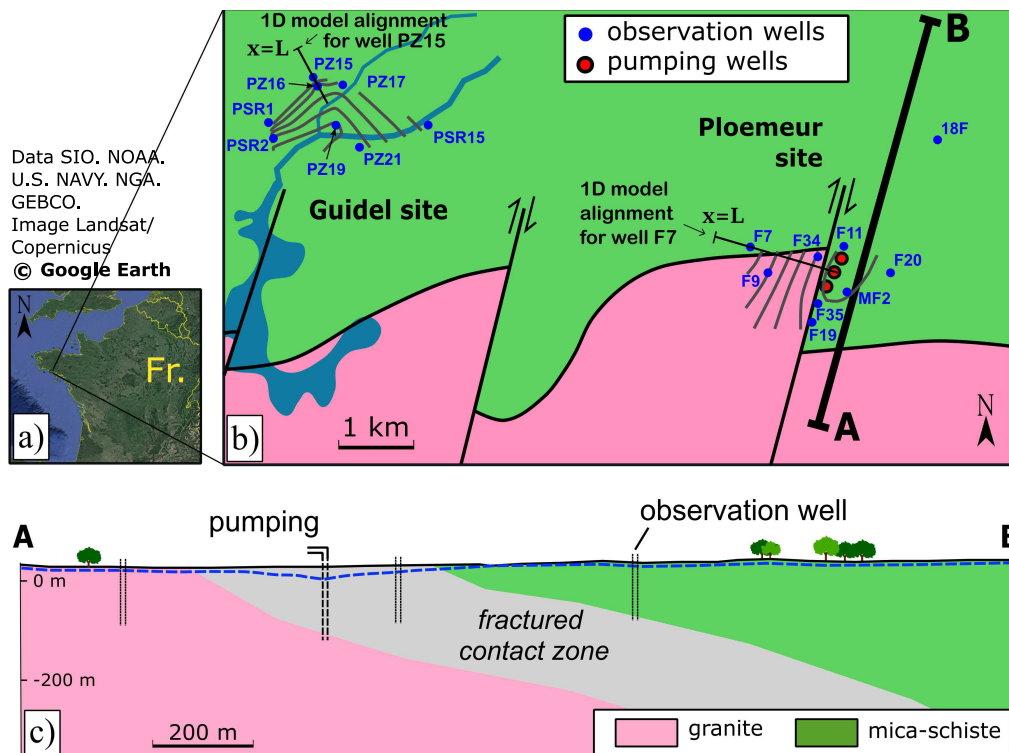


**Figure 2.** Schematic of Ploemeur and Guidel sites: a) Field sites location in France; b) Geological map and location of monitoring (blue points) and pumping wells (red points) (modified from (Ruelleu et al., 2010)). Mean GW level measured over the piezometric network is represented by gray equipotential lines. For each site, one 1D model is illustrated by a black line; c) South-North cross section of the Ploemeur site. Wells are generally screened over depths ranging from 30 to 100 m.

225 Crystalline rocks are generally considered as impermeable. However, several examples show high-yielding aquifers, which are mostly explained by the presence of fractures and weathered porous structures (Roques et al., 2016; Bense et al., 2013;



Wyns et al., 2004). Ploemeur site is a striking example as the site has been producing more than  $1 \text{ Mm}^3.\text{yr}^{-1}$  of water since 1991. The high yield of the Ploemeur aquifer is explained by the presence of a contact zone between granite and micaschist, which is highly fractured and gently dipping towards North (Fig. 2). Such structures are preferential pathways for water, which also allow drainage of a wide region beyond the topographic catchment (Ruelleu et al., 2010; Touchard, 1999; Leray et al., 2012; Jimenez-Martinez et al., 2013). The thickness of the weathered zone varies from 0 to 30 m. Several studies highlighted the heterogeneity within the Ploemeur observatory through boreholes experiments (Le Borgne et al., 2006, 2007; Dewandel et al., 2014) or water chemistry monitoring (Roques et al., 2018). Local investigations at the borehole scale also show that deep fractures can be well connected with surface. For instance, recent temperature monitoring suggests that deep fractures (80 meters deep) may be very sensitive to recharge (Pouladi et al., 2021).

On the Ploemeur site, more than 25 wells are monitoring groundwater levels since 1991. These wells are generally  $\sim 100 \text{ m}$  deep and screened over depths ranging from [30 – 100] m. As these wells are mostly localized in the vicinity of the pumping site (at a distance  $< 700 \text{ m}$ ), i.e. close to the aquifer outflow, they provide a partial view on the aquifer behavior (Roques et al., 2018). GW is extracted by three pumping wells close to the contact between micaschist and granite (north of the southern granitic outcrop) and aligned along a N20E direction (Fig. 2). The pumping wells are distant of around 50 m. Pumping rates were measured weekly from 1991 to 1997, daily since 1997, hourly since 2015. Mean GW abstraction stabilized at  $3000 \text{ m}^3.\text{day}^{-1}$ , with a seasonal variability around 15 % due to local demand increase during summer. Pumping creates a radial flow structure over a few hundreds of meters, stretched along the N20E direction. Flow structure becomes unidirectional (1D) over the remaining system ( $\sim 2 - 3 \text{ km}$  long) (Leray et al., 2012), so that flow convergence can be neglected at aquifer scale (Fig. 2). Therefore, the 1D assumption required by the analytical model can be valid at the hydrogeological system scale (Fig. 2).

The Guidel site (Bochet et al., 2020) is located 4 km west of the Ploemeur site (Fig. 2) in the same geological context. GW levels are much closer to the surface, especially in convergence zones (downstream borehole PZ19), so that hydraulic gradients are more controlled by topography. GW discharges to rivers and a wetland (Fig. 2).

### 3.2 Models setting up

Conceptually, each monitoring well intercepts a flow line between two distant boundary conditions. For the pumping site (Ploemeur site), the coordinate  $x$  of each monitoring well corresponds to its actual distance to the pumping barycenter, defined as the geometric midpoint between the three pumping wells weighted according to pumping rates. At  $x = 0$ , we impose transient pumping rates. At  $x = L$ , we assume a constant hydraulic head (blue case on Fig. 1) representing typically a river in a neighboring hillslope. Thus, the upstream area of the pumping is not fixed.

For the natural case study (Guidel site), each monitoring well is part of one hillslope bounded by a river at  $x = 0$  and bounded by another hillslope at  $x = L$ . So, the boundary condition in  $x = L$  should be a no flow condition. But similar to Ploemeur, we considered a constant head at  $x = L$  corresponding to another hillslope boundary. Thus,  $x = L/2$  would correspond more or less to the watershed divide between two hillslopes. This condition allows the watershed divide to move along  $x$  seasonally. Here, river level is shallow (typically 10 – 50 cm) and represents conceptually a constant head, as suggested by limited WTF



observed at borehole PZ19 close to the river (Fig. 3). In such context, the assumption of imposed constant head at  $x = 0$  is reasonable (boundary conditions colored in green on Fig. 1).

### 3.3 Groundwater level data

While first GW level data in Ploemeur dates back to 1991, we focus our analysis on the 1996-2017 period to avoid potential transient responses to the pumping setup. On the Guidel site, data is available from 2009 to 2017. Water levels are recorded at minute to daily time steps and decimated to daily time scales for our analysis. Hydraulic heads measured in boreholes are corrected from atmospheric pressure variations.

In Ploemeur, GW levels are relatively deep due to the pumping (depth  $\sim 7$  to  $30$  m, see Figure C1) but still contain seasonal and interannual variability (Fig. 3) due to both pumping and climate variations. Note that WTF in Ploemeur boreholes have quite similar patterns. Seasonal variations decrease with the distance to the pump: amplitude is  $5$  m at well F11,  $2.5$  m at F7 and  $1$  m at 18F, respectively at a distance of  $\sim 20$  m,  $700$  m and  $1000$  m from pumping wells.

Conversely, transient variations in response to rainfall and water cycle vary significantly among boreholes in Guidel (lower graph on Fig. 3). WTF are fairly stable for low elevation wells located close to the GW outflow (PZ19 and PZ21). On the contrary, monitoring wells located at the top of basin (PSR1, PSR2, PZ15, PZ16 and PZ17) exhibit larger seasonal variability - but still smaller than in pumped context.

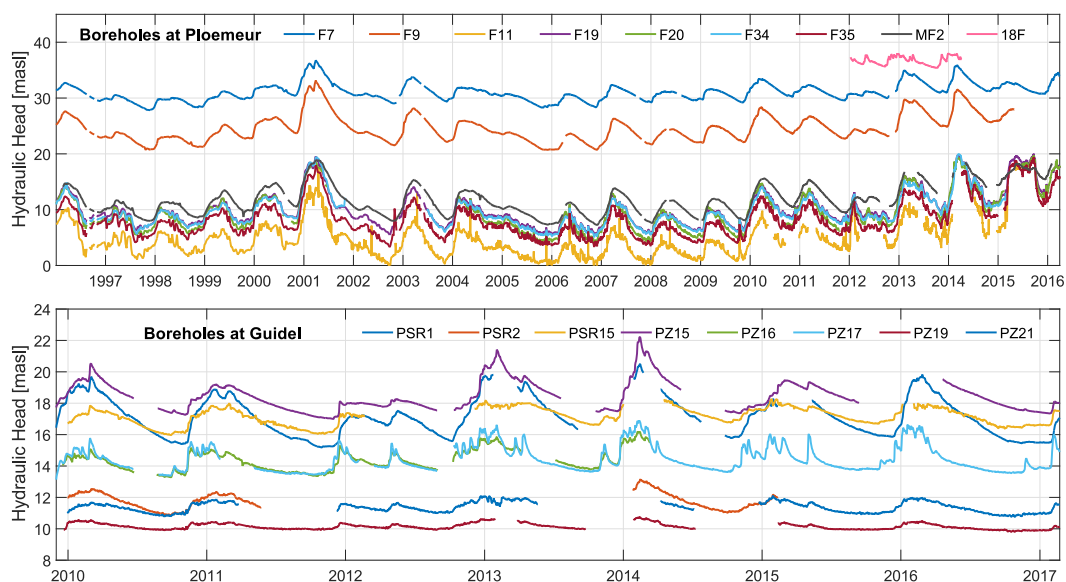


**Figure 3.** Observed GW level variations in boreholes at Ploemeur (upper graph) and Guidel (lower graph) observatories. Note the difference in scales between the two sites.



### 3.4 Climate data

A national weather station (METEO-FRANCE) is located in between the two study sites. It provides daily precipitation and Penman-Monteith potential evapotranspiration (PET) estimates. Both are used to generate potential recharge from "Thornthwaite" and GR4J soil models (next section). Within the studied period (1996-2017), annual precipitation ranges from 600 to 1100  $mm.yr^{-1}$  (mean of 880  $mm.yr^{-1}$ ) with limited variability (standard deviation of 120  $mm.yr^{-1}$ ). Rainfalls have a low seasonal variability even if 45 % of rainfalls occur between October and January. PET ranges from 670 to 890  $mm.yr^{-1}$  with a mean of 760  $mm.yr^{-1}$  with lower variability (standard deviation of 50  $mm.yr^{-1}$ ). PET has a strong seasonal variability, with mean values going from 0.6  $mm.d^{-1}$  in December and January to 3.6  $mm.d^{-1}$  in June and July.

### 3.5 Potential recharge estimates

Within the studied period, mean potential recharge rates derived from "Thornthwaite", GR4J and SURFEX models are respectively 242, 320 and 246  $mm.yr^{-1}$  i.e. 28, 37 and 28 % of rainfall (Fig. 4). Thus, Thornthwaite and SURFEX models provide similar annual amplitudes while amplitude is 30 % higher in average for GR4J (voluntarily uncalibrated). Such values are typical of Brittany given the precipitation rate and climate (Martin et al., 2006; Leray et al., 2012, 2014; Molénat et al., 1999). For the Thornthwaite model, annual potential recharge rate range from 0  $mm.yr^{-1}$  in 2002 to 600  $mm.yr^{-1}$  in 2001, representing 0 to 50 % of annual rainfall.

Recharge typically occurs from December to March. Modeled potential recharge rates, as simulated by three different soil models, remain highly variable (Fig. 4). The Thornthwaite model (in blue on Figure 4) generates episodic potential recharge events resulting from high intensity rainfall. Daily events are in average more intense for Thornthwaite model compared to GR4J (31 % smaller) and SURFEX (40 % smaller). Indeed, GR4J and SURFEX modeled potential recharge events are more diffuse with earlier events late autumn (Oct-Nov) associated to high rainfall rates. GR4J model also generates episodic recharge events in summer period linked to high rainfall intensity (summer storms).

## 4 Results

This section describes results obtained by applying and calibrating the 1D GW model to the two study sites (step 1 on Figure 1). We focus here only on water table fluctuations. The steady-state part of equation 1 (developed in Appendix A.1 and A.2) is described in Appendix C.

### 4.1 Modeling WTF across the parameters set

This part synthesizes results of the parameter space exploration for the Ploemeur and Guidel sites. Observed and modeled WTF are compared at different boreholes (see boreholes location on Figure 2 b).

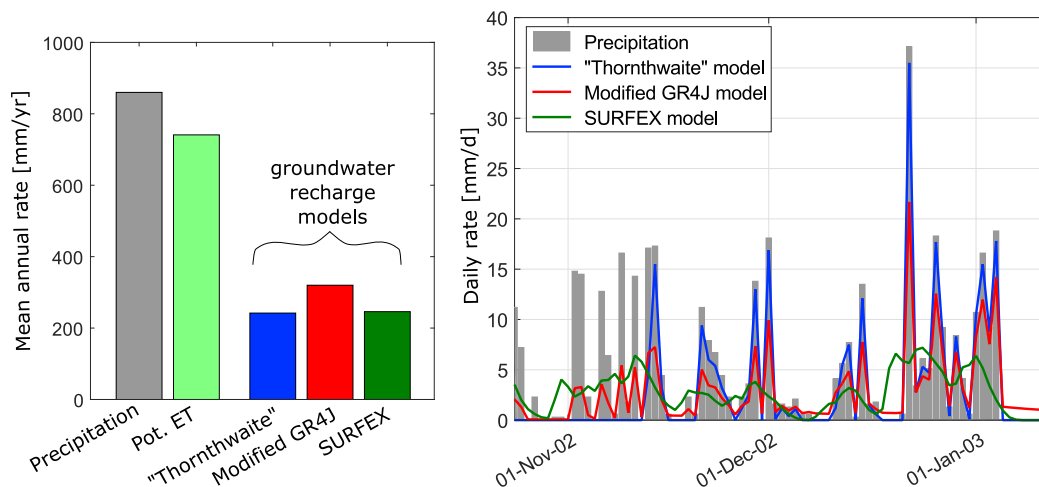


**Figure 4.** On the left: mean annual precipitation, potential evapotranspiration rate, and estimated potential recharge rates from Thornthwaite, GR4J and SURFEX models on Ploemur-Guidel sites (1996-2017). On the right: estimated daily potential recharge rates from Thornthwaite, GR4J and SURFEX models from November to January 2003. Daily precipitation are represented by grey shaded bars.

#### 4.1.1 Modeling WTF with pumping conditions: Ploemur site

305 Overall, the 1D GW model seems satisfactory when comparing observed and best modeled WTF for the Ploemur site (Fig. 5), whatever the imposed RF. Corresponding model parameters, as well as impact of imposed recharge model, are described in the next section and illustrated on figure 6. For well F9, *RMSE* criteria is lower than 0.8 m, i.e. a factor 2.5 better than standard deviation of observed WTF in this well (it corresponds to *nRMSE* of 0.4). While some wet or dry years are less well represented, seasonal to interannual variability is well modeled for all wells along the study period.

310 Best *RMSE* for each borehole is increasing when getting closer to the pumping zone: ~ 0.5 m at well F7, 0.7m at F9, 1m at MF2, and up to 1.2 m for well F11 which is 20 m away from the main pumping well. High frequency fluctuations linked to daily to weekly pumping rate variations are not well described (see WTF at F19 on Figure 5). Such a result is explained by a lack of accurate pumping data. It also highlights that the GW model fails to reproduce simultaneously short time scale fluctuations driven by pumping and seasonal to annual fluctuations.

#### 315 4.1.2 GW parameters sensitivity analysis

All parameters are not equally well determined (Fig. 6). For some parameters, the relation between model performance and parameter value shows a unique minimum indicating that the parameter is constrained by observed WTF. Characteristic time, storage coefficient and also transmissivity to model length ratio appear well constrained and quite similar between the different boreholes. For each borehole, we estimate parameters uncertainties by computing model performance on WTF (*nRMSE*) and

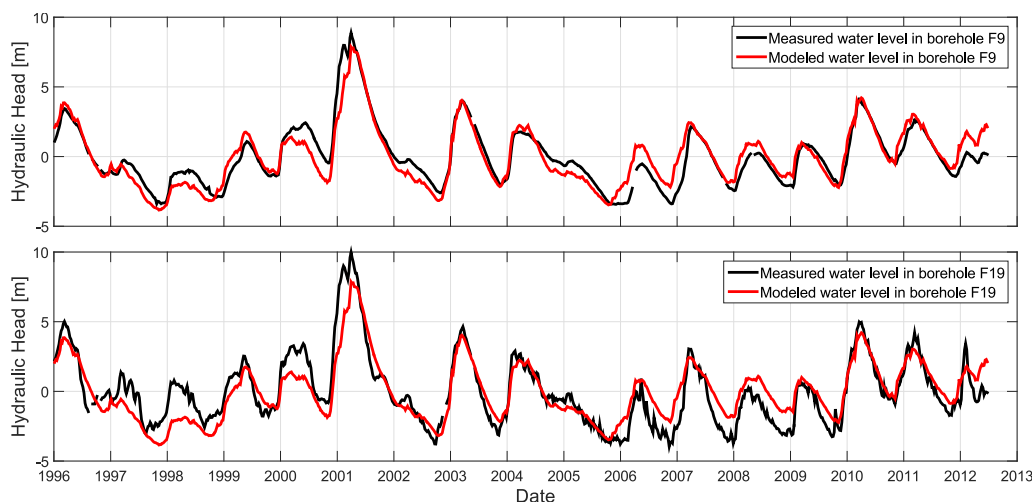


**Figure 5.** Comparison between best modeled and observed water table fluctuations at borehole F9 (upper graph) and F19 (lower graph), respectively at 519 m and 268 m of Ploemeur’s pumping wells. Parameters used correspond to best parameters (lowest *RMSE* on Figure 6 regarding water table fluctuations). Prescribed recharge fluctuations have negligible impact on these parameters and the quality of the fit.

320 fitting a normal distribution to the curves presented on Figure 6. Optimal parameter and uncertainty are defined as the mean and standard deviation of this normal distribution.

Estimated characteristic time (Eq. 2) is equal to 1.5 *yr* and ranges between 0.3 to 7.6 *yr* among different boreholes (top-left on Figure 6). Optimal values range from 1 – 2 *yr* among different boreholes. Moreover, parameter estimation appears independent of prescribed potential recharge. This is highlighted at borehole F7 (black line) on figure 6: the variability induced  
325 by the choice of the prescribed potential recharge model (grey shaded area) is very limited. Thus, recharge volumes uncertainty (Fig. 4) has a limited impact on parameters estimation.

Interestingly, storativity is also well constrained as  $S \in [2 \times 10^{-2}; 1.3 \times 10^{-1}]$  with a mean value of  $5 \times 10^{-2}$  (see top-right on Figure 6). But *S* is more variable among the different wells as compared to characteristic time. The analytical solution (Eq. 2) shows that *S* participates in the overall amplitude of the well reaction to recharge, linked to recharge volume for each frequency.  
330 Storativity is slightly affected by uncertainties in prescribed recharge volumes (illustrated by grey shaded area at borehole F7 on figure 6). Conversely, transmissivity and aquifer length are poorly estimated, mainly because they can compensate each other ( $L/T$  appears explicitly in equation 2).

#### 4.1.3 Results and sensitivity analysis for Guidel site

Similarly to Ploemeur, the analytical GW model manages to describe adequately WTF at Guidel (Fig. 7) although WTF  
335 patterns are very different (Fig. 3). Note we used the same potential recharge from Thornthwaite as in Ploemeur. For well PZ15, *RMSE* is 0.4 m, i.e. ~ 40 % of the standard deviation of observed fluctuations. More generally, the model explains 40 to 60 % of the WTF variability (right graph on Figure 7), with *RMSE* around 0.4 m for wells located upstream, while

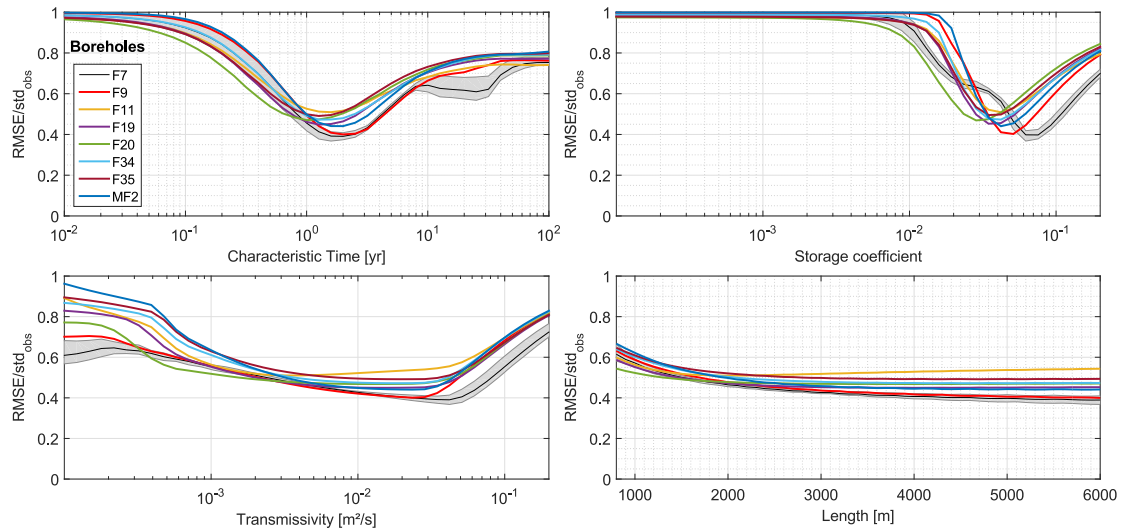


**Figure 6.** Evolution of the minimal normalized  $RMSE$  for Ploemeur wells as a function of model parameters: characteristic time (top-left), storage coefficient (top-right), transmissivity (bottom-left) and aquifer length (bottom-right). We selected the best prescribed potential recharge model for each point. The impact of the prescribed recharge is drawn by the shaded area on borehole F7.

limited to  $0.1 - 0.2 \text{ m}$  for wells located near the lower boundary condition (PSR15, PZ19, PZ21). Overall, model performance is slightly lower on Guidel than on the Ploemeur site. Therefore, model parameters are also less constrained. Characteristic times are close to those obtained in Ploemeur, but with a wider range of  $0.3 - 50 \text{ yr}$  (Fig. 7). Estimated storage coefficient ranges from  $3 \times 10^{-2}$  to  $1.5 \times 10^{-1}$  and transmissivity from  $10^{-4}$  to  $5 \times 10^{-3} \text{ m}^2 \cdot \text{s}^{-1}$ . Aquifer length is poorly defined and closely linked to transmissivity as for the Ploemeur site.

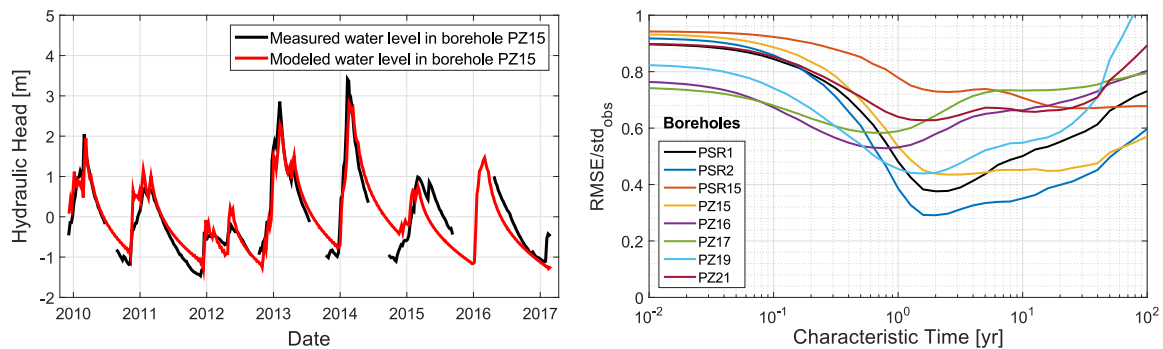


**Figure 7.** Comparison between best modeled and observed water table fluctuations at borehole PZ15 in Guidel (left). Evolution of the minimal normalized  $RMSE$  as a function of characteristic time for Guidel boreholes (right).



## 5 Recharge fluctuations estimate from observed WTF

### 5.1 Summary of the parameter space exploration

345 In the previous section, we showed that a simple GW model that neglects aquifer heterogeneity can well reproduce observed WTF. An important result is that estimated hydrodynamic and geometric parameters are independent of prescribed potential recharge models (Fig. 4). They also appears quite independent of individual WTF (Fig. 6). These parameters define lateral GW flow. So, the model can be further exploited to infer recharge from WTF observed in different boreholes. For each borehole, RF are estimated using parameter values from the 5 % best models.

350 Note that transmissivity is not well defined from temporal fluctuations. Mean water table in each borehole is impacted by heterogeneity (Figure C1 in Appendix C). As a consequence, mean (long-term) recharge cannot be accurately computed (see the steady-state term in equation A8). However, RF, defined as recharge variations (or anomalies) with respect to the long term mean, are fully reachable. In addition, even if parameters uncertainties can strongly impact the range of RF estimates (Appendix B), aquifer parameters ( $T$ ,  $S$  and  $L$ ) compensate each other through model calibration such that characteristic time  
355 remains the most important parameter. Since characteristic time is obtained with a small uncertainty, its uncertainty has little impact on RF estimates (Appendix B).

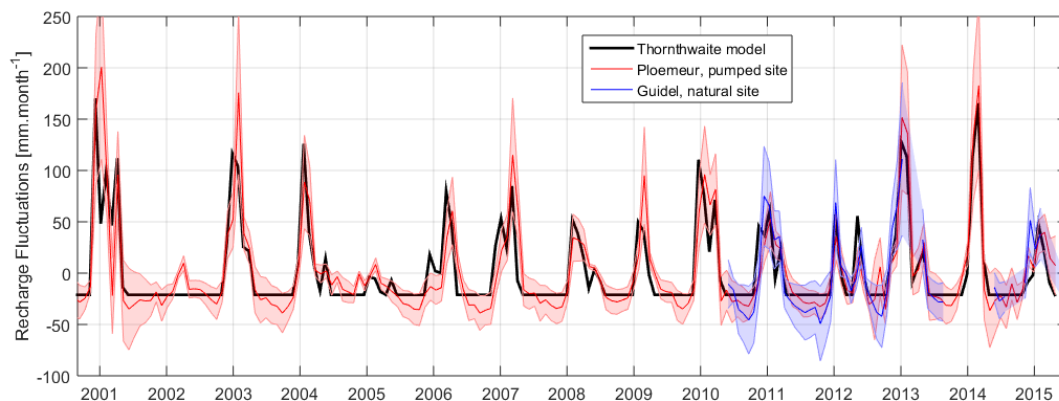
### 5.2 Recharge fluctuations estimate for Ploemeur and Guidel sites

The analytical GW model appears as a low-pass filter in equations 2 and 3, smoothing out high frequency pumping and recharge variability (these variables are divided by frequency in equations 2 and 3). In the backward modelling (Eq. 5 and  
360 6), any high frequency WTF variability is therefore amplified to recompute recharge. In order to reduce noise amplification linked to observation uncertainties, particularly for boreholes close to the pumping zone, and to facilitate plots reading, RF are inter-compared at monthly time scale.

Phase and amplitude of RF are quite similar between the different wells (Fig. 8). Recharge noise increases when the borehole is well connected to the pumped fractured zone, as suggested by difference in RF between  $F9$  and  $F19$  (SI), respectively 519  
365  $m$  and 268  $m$  far from the pumping station. This can be expected as observed WTF contain high frequency variations linked to short-term pumping rate variations, which are difficult to model (Fig. 5). It only impacts high-frequency variations for some boreholes.

Overall, RF estimated "from above" and RF performed with the GW analysis agree well at seasonal to long-term time scales. Main differences appear at monthly times scales. On the Ploemeur site (respectively Guidel), the Thornthwaite model  
370 overestimates RF temporal variability obtained analytically from well F7 (respectively well PSR1) by 40 % (respectively 20 %), while both GR4J and SURFEX models fall within 5 – 6 %. In terms of the succession of recharge events, correlation is 0.55, 0.58 and 0.65 for Thornthwaite, GR4J and SURFEX respectively, on Ploemeur site. In general, Thornthwaite potential recharge events are  $\sim 15$  days ahead as compared to inverted RF on Ploemeur site, and slightly ahead with respect to the Guidel site. SURFEX performs better than other potential recharge models, better predicts all effective recharge events during  
375 dry years (2002, 2005) and wet summers (2004, 2012), but fails in describing intense recharge events.





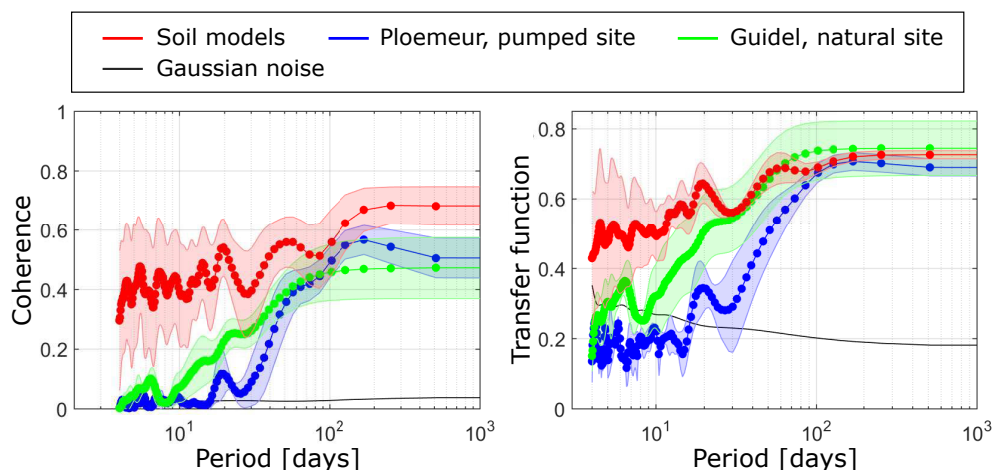
**Figure 8.** Monthly recharge fluctuations estimated from GW analytical model at different boreholes on the Ploemur (in red) and Guidel (blue) sites, propagating model parameter uncertainties. Black line represents potential recharge fluctuations (anomalies compared to the mean value) from the Thornthwaite model.

Figure 8 shows analytically estimated RF for both Ploemur and Guidel sites, including uncertainties linked to parameters uncertainty. Although WTF are very different on each site (Fig. 3), estimated RF are highly coherent in both cases. On average, Thornthwaite model overestimates analytically estimated RF by 10 to 20%. Though, on a few events, analytically estimated RF can be larger. Based on these results, we can assert that recharge events greater than  $25 \text{ mm.month}^{-1}$  can be detected with this method, as highlighted by single events that occurred in winter 2002 and 2005.

### 5.3 The unsaturated zone and recharge fluxes

On figure 9, the coherence and transfer functions (Eq. 7 and 8) between  $P - PET$  fluctuations and RF describe unsaturated zone behavior and inform on the transformation of rainfall events into recharge. This is a a proxi of rainfall efficiency. Inverted RF at both study sites (in blue and green on Figure 9) and potential RF (in red) are highly coherent with  $P - PET$  fluctuations (i.e. significantly larger than the expected coherence of Gaussian noise) over a wide range of frequencies, especially for periods larger than 100 days. The amount of  $P - PET$  that recharges GW varies from  $< 20 \%$  at small temporal scales to  $> 75 \%$  at long-term time scales (typically seasonal time scale with winter rainy season).

Soil models generally fail to describe  $P - PET$  efficiency to recharge GW at smaller time scales. Indeed, after episodic events, modeled potential recharge from three soil models (in red on Figure 9) occurs more rapidly and with larger amplitudes as compared to RF inferred from observed WTF (in blue and green on Figure 9). On the Ploemur site,  $P - PET$  efficiency to recharge GW seems to be negligible (i.e. below the noise level) at periods below  $\sim 30 \text{ days}$ , and climbs to maximum values for period  $> 100 \text{ days}$  (in blue on right graph on Figure 9). Interestingly, coherence and rainfall efficiency in Guidel (in green on Figure 9) are rising much earlier than in Ploemur, beginning  $\sim 10 \text{ days}$  periods. This underlines a tighter link between  $P - PET$  and GW recharge in Guidel and a higher sensitivity to rainfall events.



**Figure 9.** Coherence (left) and Transfer function (right) between  $P - PET$  and RF estimated from observed water table on Ploemeur and Guidel sites or between  $P - PET$  and potential RF obtained from soil models (Thornthwaite, GR4J, SURFEX). The transfer function of a  $25 \text{ mm} \cdot \text{month}^{-1}$  Gaussian noise is given as a reference.

395 Figure 9 shows that rainfall events distribution throughout the year impacts RF because the transfer function between  $P -$   
 $PET$  fluctuations and RF inferred from WTF is basically frequency dependent. Intense rainfall events can generate recharge  
pulses through the unsaturated zone which will be diffused through the aquifer. Indeed, a single rainfall event is mathematically  
equivalent to a Dirac impulsion, which Fourier transform has a constant amplitude on all frequencies. The efficiency of such  
single rainfall events is therefore distributed on the whole spectrum, meaning that each rainfall event which is not consumed  
400 by evapotranspiration will necessarily be translated into recharge. Finally, recharge can occur during both (1) long/sustained  
winter rainfall and (2) episodic/intense rainfall events. We can also expect that recharge resulting from intense rainfall events  
will be more pronounced on Guidel site as efficiency increases earlier at small temporal scales (i.e. thinner unsaturated zone).

Overall, potential RF and RF estimated from WTF can be described by a linear behavior when integrated at annual time step,  
but significant deviations exist in terms of amplitude and variability. Thornthwaite RF equals 92% of wet-season  $P - PET$ ,  
405 while RF from observed WTF would suggest a range between 68 – 74% on the pumping site, and 77 – 110% on the natural  
site where GW level is close to the surface. On Ploemeur site, the amount of seasonal recharge is therefore much lower than  
expected with the Thornthwaite model, while it can be larger on Guidel site.



## 6 Discussion and consequences

### 6.1 The parsimonious strategy constrains well hydrogeological characteristics

#### 410 6.1.1 Aquifer characteristic time constrained by aquifer characteristics : $T$ , $S$ and $L$

Here, we originally inferred GW properties based on WTF measured in boreholes. These fluctuations generally bear typical frequencies from climatic and anthropic boundary conditions (hourly rainfall event, small diurnal variations due to evapotranspiration fall during the night, seasonal human water consumption, climatic cycles...). They are also linked to the characteristic time of the system, and consequently to spatial scale. A first outcome of this work is that a simple physically-based GW model can explain WTF at the scale of the piezometric network although local geological heterogeneities can play an important role, as shown in the steady-state case on Appendix C or by daily to monthly pumping tests (Le Borgne et al., 2006). Correlation among well observations due to lateral GW flow brings insights into the aquifer averaged characteristic time. A second outcome is that inferred equivalent hydraulic and geometric parameters are similar among boreholes and close to those obtained by previous modeling studies investigating the overall behavior of Ploemeur site, including a spatially-distributed approach (Leray et al., 2012). This provides confidence that the general aquifer behavior is well captured and that inferred parameters have some physical meaning.

Aquifer characteristic time ( $L^2S/T$ ) controls how the distribution of recharge events is transferred laterally. Here, estimated characteristic time is typically 1.5 *yr*. However, model length  $L$  is here a proxy of the distance between two streams. Considering that the model can be decomposed in two hillslopes of length  $L/2$ , feeding rivers in  $x = 0$  and  $x = L$ , would reduce characteristic time to around 5 *months*. Such times appear short regarding the crystalline aquifer context. They appear much shorter than GW response time estimated from worldwide parameters map in Cuthbert et al. (2019a) and than "time to reach equilibrium" estimated for the biggest world aquifers in Rousseau-Gueutin et al. (2013). However, characteristic length is here much smaller and constrains characteristic time (Bresciani et al., 2016; Gauvain et al., 2021). Such estimates are in line with aquifer characteristic times typically inferred from streamflow and water quality data in the region (Guillaumot et al., 2021).

Here, storage coefficient values ( $2 \times 10^{-2} - 1.5 \times 10^{-1}$ ) are similar to those obtained in previous studies:  $S$  was ranging from  $5 \times 10^{-3}$  to  $5 \times 10^{-2}$  for a recharge of 260 *mm/yr* (Jimenez-Martinez et al., 2013) or from  $2 \times 10^{-2}$  to  $6 \times 10^{-2}$  for a recharge of 200 *mm/yr* (Leray et al., 2012). Such values are much larger than expected for a crystalline context, and larger than typical estimates from short-term pumping tests, where  $S$  was ranging from  $10^{-5}$  to  $10^{-2}$  (Le Borgne et al., 2006). Storage coefficient estimates typically depend on the length of the study period (SI), so that WTF should be used on periods longer than 1 *year* typically for the Ploemeur and Guidel sites. This study, mostly based on seasonal time scales, suggests that part of the confined fractured aquifer is well connected to a more porous aquifer functioning as a storage compartment. Further discussion on this point can be found in Jimenez-Martinez et al. (2013).

In this work, transmissivity is estimated in the range  $T \in [8 \times 10^{-4}; 8 \times 10^{-2}] m^2.s^{-1}$  (Fig. 6), such large ranges are also found in previous studies, e.g.  $T \in [4 \times 10^{-3}; 4 \times 10^{-2}] m^2.s^{-1}$  in Jimenez-Martinez et al. (2013) and Le Borgne et al. (2006). Leray et al. (2012) calibrated a 3D model and defined a constant transmissivity  $T = 2 - 3 \times 10^{-3} m^2.s^{-1}$ . Note that "local"



transmissivity can be better estimated from pumping tests - which typically lasts several hours to several months, while storativity is highly affected by heterogeneity during such experiments (Le Borgne et al., 2006; Meier et al., 1998). This highlights the tight link between estimated hydraulic parameters and predominant boundary conditions at the time scale of the study (Cuthbert et al., 2019a).

#### 445 **6.1.2 On the representativity of GW levels**

We found that WTF observed in boreholes contain the overall aquifer response for observation periods around and larger than the aquifer characteristic time. However, the steady-state approach shows the difficulty to bring relevant aquifer-scale information from mean GW levels because of local heterogeneities, incomplete sampling of the GW system and high sensitivity to model assumptions (Appendix C). Thus, heterogeneity largely impacts the ability to estimate mean GW recharge rate from  
450 GW levels while RF over time generate lateral GW flow that links different GW head observations. For this reason, a single well contains information on aquifer-scale recharge, as underlined in the WTF approach (Cuthbert, 2010; Healy, 2010; Cuthbert et al., 2016, 2019b). Though, the WTF method alone has some limitations. We show that the well position within the GW flow system is as important as storativity to define recharge (geometric term in equation 5). Indeed, as recharge is transferred laterally, downstream wells will integrate the impact of both local and upstream recharge. Such behavior is expected to be  
455 even more pronounced if the well is located in a convergence zone (2D behavior). To go further, evapotranspiration losses in downstream area could be inferred from boreholes located in upstream area. This is probably already the case in Guidel, thus RF would correspond to net RF. Finally, knowing the spatial variability of aquifer properties could be unnecessary to model groundwater systems and fluxes between hydrological compartments.

#### **6.1.3 Limitations**

460 The main assumptions of the model are (1) the 1D lateral flow structure, (2) homogeneous GW parameters and (3) uniformly distributed recharge. Regarding the 1D assumption on Ploemeur, pumping controls aquifer behavior so that 1D assumption is valid over the system except close to the pumping wells. Pumping has generated a GW flow structure more or less constant for 25 *years*. Water table does not interact with the surface. In this case, aquifer characteristic time is perfectly constrained and not borehole dependent. On Guidel, GW intercepts locally the ground. Therefore, the flow structure is mainly driven by topography  
465 and is more complex as highlighted by the different WTF patterns (Fig. 3). In this case, the system can be considered as a set of 1D hillslope models. However, in Guidel, GW flow direction should be modified between seasons at boreholes close to rivers and wetland making the 1D assumption less reliable. More generally, nonlinear GW-surface interaction (more pronounced during extreme dry or humid events) prevent to reproduce WTF in such boreholes using 1D models. Indeed, model performance is limited for a few wells located close to rivers (PZ21, PSR15, PZ17), but agree well for other boreholes in the western part,  
470 where aquifer characteristic time seems to converge (close to 1.5 *yr*).

We assume that the heterogeneous system may be described by equivalent hydrodynamic properties. Previous works have highlighted that the behavior of complex aquifers could be described by equivalent homogeneous models when focusing on specific spatial and temporal scales (Clauser, 1992; Rovey and Cherkauer, 1995; Jimenez-Martinez et al., 2013; Herzog et al.,



2021) or for well connected fracture networks at large scale (Liu et al., 2016). While GW heterogeneity cannot be accurately  
475 captured and then represented in GW models, our results show that it was not necessary to add complex geological structures  
or consider a 2D geometry to well describe observed WTF in most of the boreholes. One limitation of this approach could be  
the effect of larger scale heterogeneity in the geology such as transitions between lithological units. Indeed, in the case where  
a complex structure would affect the equivalent aquifer properties in function of time, the analytical models will not be able to  
include such behavior.

480 The assumption of uniform recharge might be seen as unrealistic considering that local topographic and geological structures  
can favor exchanges between surface and groundwater (Favreau et al., 2009; Appels et al., 2015). It should be noted that the  
recharge period typically lasts 4 to 5 months, while GW flow behaves as an integrative (smoothing) system with typical time  
integration scale  $\sim 1$  year, smoothing out high frequency pumping and recharge variability. In these conditions, it is expected  
that the deviation of recharge distribution does not alter the estimation of system-scale RF.

485 Finally, note that the forward and backward analytical models can be run at any – and different – time steps. The heart of the  
model is in frequency domain, so that the first step consists in computing a Fourier transform to define amplitudes over a series  
of cosine functions. The number of frequencies is limited by the WTF sampling (Nyquist frequency). The recomposition in  
temporal domain requires to sum again cosine functions, but all frequencies do not need to be used, and the temporal sampling  
can be adapted. This flexibility is a real strength, but some numerical issues can arise. High frequencies in potential recharge are  
490 damped when modelling WTF (equations 2 and 3), so that high frequency uncertainties have a limited impact. Conversely, in  
the backward model, observed WTF ( $\bar{h}(x_r, \omega)$ ) are multiplied by frequency (equations 5 and 6) so that any high frequency error  
(or noise) in observed WTF will be amplified in RF estimation. To avoid such issues, we used temporal averaging in temporal  
domain to mitigate such noise amplification, but alternative methods can be used. Thus, applying the method requires time  
series of water levels at time steps appropriate for meeting study objectives. To reduce computing time, parameter calibration  
495 can be done at bigger time step, thus potential recharge estimate can be provided at this bigger time step. Here, we did it at  
weekly time step while RF are computed from daily WTF. We highlights that potential recharge can be a rough estimate or a  
first guess of RF.

## 6.2 Groundwater data informative content on recharge dynamics

We stated that uncertainty on potential RF was not critical to estimate GW parameters from long-term observed WTF. There-  
500 fore, the GW model was analytically inverted based on inferred parameters and observed WTF to investigate recharge pro-  
cesses. We highlighted that the seasonal GW recharge signal seems integrated whatever the borehole location within the  
heterogeneous aquifer.

### 6.2.1 Seasonal recharge fluctuations

In this work, we directly compared recharge derived from GW levels analysis with potential recharge estimates typically  
505 formulated by large-scale or conceptual soil models. Overall, potential recharge estimated from soil models and recharge  
inferred from GW levels are fairly equivalent at seasonal to long-term time scales on the both sites but they differ from short



to mid-term (< season) scale (Fig. 9). The tested soil models lack realism at short temporal scales (typically below 3 months), where recharge is often overestimated. Soil models are found to be too reactive to rainfall events and they lack storage capacity.

The dependence of GW recharge to rainfall intensity and distribution throughout the year has been documented in several studies (Barron et al., 2012; Kendy et al., 2004; de Vries and Simmers, 2002; Gee and Hillel, 1988; Taylor et al., 2012). The same behavior is well demonstrated in this study, where annual RF amplitude cannot be fully expressed as a fraction of annual rainfall (see also Collenteur et al. (2021)). For example, total  $P - PET$  during humid period is around 400 mm for different years, though, analytically estimated RF can differ by more than 100 mm. The classical approach consists in defining statistics on the distribution and intensity (e.g. number of days without rain, cumulative sorted rainfall), but does not often yield satisfactory results. Considering the relationship between  $P - PET$  and recharge as a frequency dependent function is a simple but effective way to consider the impact of rainfall distribution on recharge. Indeed, this function defines the relative efficiency to generate recharge between a single rainfall event and a long-lasting wet season, and has been recently tested by Schuite et al. (2019). Based on RF estimated from WTF, we highlight that the frequency-dependent relationship between  $P - PET$  and recharge can be described as a combination between a high-pass and a low-pass filter, which could represent the respective contribution of macropores and vertical unsaturated flow to recharge. It describes how both long period seasonal rainfall and intense events participate significantly to recharge. Additional development should be carried out to link the shape of the transfer function (efficiency at high and low frequencies, cutoff frequencies) to the structure and hydrodynamic parameters of the unsaturated zone.

## 6.2.2 Partitioning of potential recharge

The proposed approach allowed computation of both RF and associated uncertainties at seasonal time scales to re-investigate the relationship between wet season  $P - PET$  and recharge. Similarly, potential RF and boreholes-estimated RF can be linked by a linear behavior. Thereby, the linear coefficient can be seen as a potential recharge partitioning coefficient. This partitioning coefficient should differ between Ploemeur and Guidel assuming their potential recharge is similar. Indeed, 74 to 80% of the potential recharge could be converted into groundwater recharge on Ploemeur site. For Guidel, this value ranges from 84 to 100%. The remaining part would be attributed to lateral flow within the unsaturated zone between the soil and the water table.

## 6.3 Pumping impacts recharge dynamics and main hydrogeological processes

### 6.3.1 Impact of the unsaturated zone thickness

The comparison between the Ploemeur and Guidel sites offers the opportunity to gain insights into the role of the unsaturated zone. On the Ploemeur site, the mean unsaturated zone thickness is  $\sim 15m$ , while limited to  $\sim 4.5m$  on Guidel site. Indeed, pumping thickens the unsaturated zone, so that potential recharge under the soil is first buffered in the deep unsaturated zone before generating GW recharge. We can infer that the unsaturated zone plays an inertial role by storing water and filtering out high frequency variability. This is confirmed when looking at frequency-dependent time lags between  $P - PET$  and recharge (not shown), which is systematically larger on the Ploemeur site than on Guidel. We showed unsaturated zone thickness does



not impact only the amount of recharge, but also the efficiency of short-term rainfall (Fig. 9). From these observations, we can  
540 conclude that setting up a pumping can decrease recharge by impacting negatively the overall contribution of episodic recharge  
events. These results are in line with Cao et al. (2016) on the North China Plains.

### 6.3.2 Change of solicited critical zone compartment from natural to pumped conditions

Inferred aquifer parameters slightly differs between the two neighboring sites although located in the same geological context.  
On average, storage coefficients are larger and transmissivities smaller on the Guidel site than on the Ploemeur pumping  
545 site. One interpretation of this result is that the weathered zone contributes more to GW flow on the Guidel site. Indeed, the  
weathered zone (0 – 20m depth), known to be more porous and less permeable, should impact more GW flow when GW levels  
are closer to the surface. Conversely, on the Ploemeur pumping site, "deep" fractured aquifer controls flow as GW levels are all  
~ 15 m below ground. While diffusivities ( $T/S$ ) are typically larger on Ploemeur, characteristic times are similar on both sites,  
meaning that the actual aquifer length  $L$  on Ploemeur is longer. As a consequence, GW flow extends beyond the topographic  
550 limits of the catchment, as it can be expected by the pumping (Fig. 1).

## 7 Conclusions

A parsimonious GW flow model has several advantages (Hill, 2006). It offers an easy understanding of simulated flow pro-  
cesses (Rousseau-Gueutin et al., 2013; Schuite et al., 2017), focusing the interpretation on the physical meaning of model  
misfit and the balance between model complexity and available data. Also, the limited execution time allows to explore the  
555 actual knowledge that could be gained from available (often sparse) observations. A central result is that a parsimonious GW  
flow model reproduces well GW level fluctuations (or anomalies) in heterogeneous aquifers once boundary conditions are  
well defined. We showed that GW level fluctuations observed in one borehole contain aquifer-scale flow information at time  
scales equivalent or larger than the characteristic response time, while time-averaged groundwater levels are sensitive to both  
boundary conditions and heterogeneity. Therefore, the impact of local heterogeneities is smoothed out so that aquifer-scale  
560 equivalent characteristic time and storage coefficient are reachable with limited dependence to prescribed potential recharge.

The developed GW models are also invertible analytically to recover boundary conditions. Indeed, we estimated groundwater  
recharge fluctuations from observed GW level fluctuations time-series. A key novelty of this approach is developing the WTF  
method in the frequency domain Townley (1995). Note the method can be used to infer mean annual recharge value. However,  
we argue this is less relevant in heterogeneous aquifer. The approach was tested on two neighboring sites, one being pumped  
565 for 25 *years*. First, estimated recharge from borehole data analysis is coherent among each borehole, on each site. Then, the  
comparison between the two sites highlights how unsaturated zone thickness affects recharge. In both cases, the response to  
rainfall is quite equivalent at time scales  $> 100$  *days*. The main difference lies at small temporal scales, the response to rainfall  
is more important when the unsaturated zone thickness is small. We finally showed how groundwater pumping mitigates high  
frequency recharge events by thickening the unsaturated zone.



570 A large uncertainty in hydrological modeling lies in the fact that GW recharge can be derived from oversimplified conceptual soil models. Such an approach as described here gives hope that the GW heterogeneity issue could be overcome in large scale models by defining the equivalent basin response with a similar frequency-domain analytical model. Note that a similar approach has been designed to model streamflow variations on a bigger basin (Schuite et al., 2019). Several analytical solutions are provided in supporting material considering either streamflow or GW level fluctuations and considering different imposed boundary conditions.

575 This method could be applied in several parts of the world where GW levels time series are available over long time scales. It could give a useful alternative to study GW flows and recharge processes and their sensitivity to imposed boundary conditions, namely, precipitations and water use.

580 *Code and data availability.* Data and Matlab models developed for this study, as well as models with different configurations, are available on <https://hplus.ore.fr/en/guillaumot-et-al-2022-hess-data>.

## Appendix A: Development of the analytical groundwater model

### A1 1D groundwater flow equation resolved in frequency domain

The 1D diffusivity equation (also called GW flow equation), under Dupuit assumption, can be written as:

$$T \frac{\partial^2 h(x,t)}{\partial x^2} = S \frac{\partial h(x,t)}{\partial t} - R(t) \quad (\text{A1})$$

585 where  $h(x,t)$  are hydraulic head variations [ $L$ ];  $R(t)$  the time-dependent, uniformly distributed recharge rate from the surface [ $L.T^{-1}$ ];  $T$  the aquifer transmissivity [ $L^2/T$ ] and  $S$  the storage coefficient of the aquifer []. Time dependent variables are then decomposed in Fourier domain:

$$f(x,t) = f_{mean}(x) + \sum Re \{ \bar{f}(x,\omega) e^{i\omega t} \} \quad (\text{A2})$$

where  $f_{mean}(x)$  is the steady state term and  $\bar{f}$  are complex Fourier coefficients depending on  $x$  and frequency  $\omega$ .  $Re$  means the real part. Note that the first term of equation A2 corresponds to  $\omega = 0$  and will be solved separately. Injecting equation A2 in equation A1 leads to the following equation for each frequency, which does not depend on time after simplification by  $e^{i\omega t}$ :

$$\frac{\partial^2 \bar{h}(x,\omega)}{\partial x^2} - \frac{i\omega}{D} \bar{h}(x,\omega) = -\frac{\bar{R}(\omega)}{T} \quad (\text{A3})$$

590 with  $D = \frac{T}{S}$

where  $D$  is the hydraulic diffusivity [ $L^2/T$ ]. The transformation of the initial partial differential equation (from time  $t$  to pulsation  $\omega$ ) leads to a simpler second order equation which admits a general solution of this form, for each Fourier mode:

$$\bar{h}(x,\omega) = A(\omega) e^{x/X} + B(\omega) e^{-x/X} + \bar{R}(\omega) \frac{X^2}{T} \quad (\text{A4})$$





with  $X = \sqrt{\frac{D}{i\omega}}$

In addition, the steady state part of equation A1 admits a range of solution of the form:

$$h_{mean}(x) = C_1x^2 + C_2x + C_3 \quad (A5)$$

595 Finally, the general solution of equation A1 is written:

$$h(x,t) = C_1x^2 + C_2x + C_3 + \sum Re\{e^{i\omega t} \left[ A(\omega)e^{x/X} + B(\omega)e^{-x/X} + \bar{R}(\omega)\frac{X^2}{T} \right]\} \quad (A6)$$

where  $C_1$ ,  $C_2$  and  $C_3$  refer to unknowns that can be determined from at least two boundary conditions.

## A2 Defining boundary conditions

In equation A1, GW recharge is taken into account as a time variable term, uniformly distributed along the  $x$  axis of the model. Boundary conditions are applied on the two boundaries of the domain of length  $L$  (Fig. A1). Boundary conditions can be constant in time and/or time variable. Boundary conditions can be of two kinds: (1) Dirichlet boundary conditions where the value of  $h$  is specified, or (2) Neumann boundary conditions where the derivative of  $h$  (i.e. flux) is specified.

The first model configuration described in figure A1.a), corresponding to the Ploemeur pumping case, is defined by the following boundary conditions:

605

- at  $x = 0$ ,  $Q(0,t) = Q_{pumping}(t) = -TW \frac{\partial h(0,t)}{\partial x}$  (from Darcy's law)
- at  $x = L$ ,  $h(L,t) = h_L$

The first condition can be decomposed in one steady-state term  $Q_{mean}$  and a sum of coefficients  $\bar{Q}$  after Fourier transform. The second condition appears as  $h_{mean}(L) = h_L$  in the steady part, which means  $\bar{h}(L,\omega) = 0$  in the time variable component. So, this leads to the next equations admitting  $A$  and  $B$  as unknowns:

$$\bar{Q}(\omega) = -\frac{TW}{X} [A(\omega) - B(\omega)] \quad (A7)$$

$$0 = A(\omega)e^{L/X} + B(\omega)e^{-L/X} + \bar{R}(\omega)\frac{X^2}{T}$$

Thus, the analytical solution for this model can be obtained once  $A$  and  $B$  are defined:

$$h(x,t) = \frac{R_{mean}}{2T}(L^2 - x^2) + \frac{Q_{mean}}{WT}(L - x) + h_L + \sum Re\{e^{i\omega t} \left[ \bar{R}\frac{X^2}{T} \left( 1 - \frac{\cosh \frac{x}{X}}{\cosh \frac{L}{X}} \right) + \bar{Q}\frac{X}{TW} \frac{\sinh \frac{x-L}{X}}{\cosh \frac{L}{X}} \right]\} \quad (A8)$$

610 The second model configuration described in figure A1.b), corresponding to the Guidel "natural" case, is defined by the following boundary conditions:

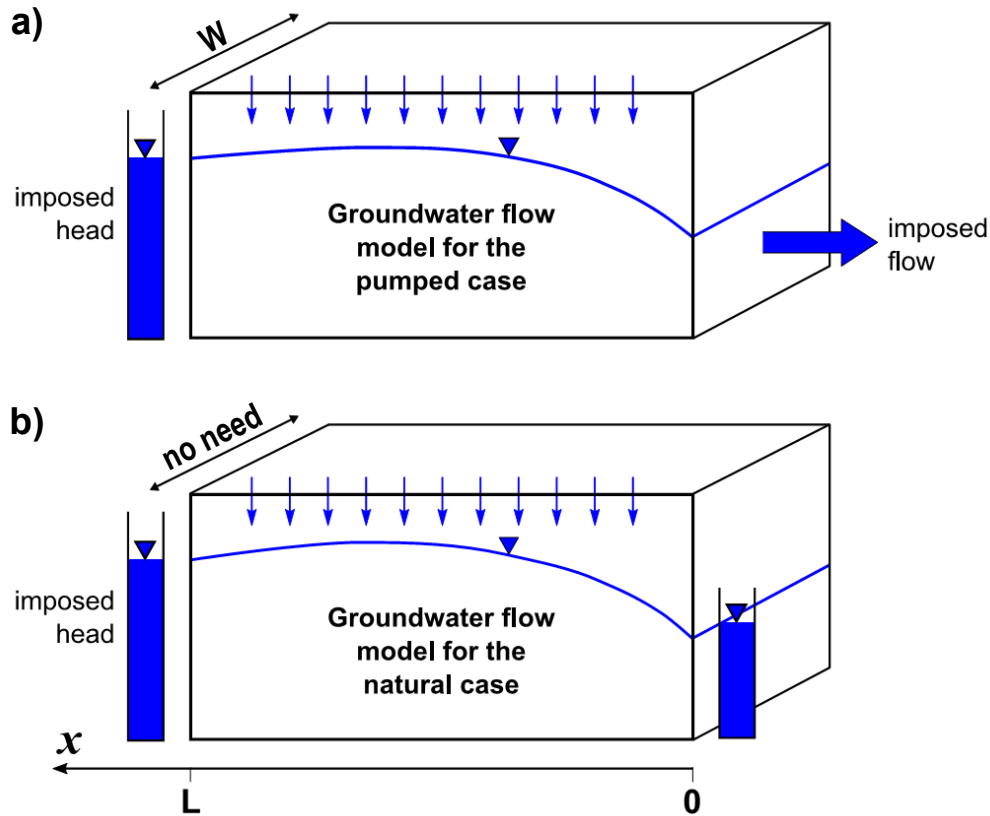


**Figure A1.** Scheme of the analytical 1D groundwater model. Hydraulic head is variable along  $x$  axis. Transmissivity  $T$  and storativity  $S$  are constant. a) With boundary conditions corresponding to the pumping case. b) With boundary conditions corresponding to the "natural" case (the solution is independent from model width  $W$ ).

- at  $x = 0$ ,  $h(0, t) = h_0$
- at  $x = L$ ,  $h(L, t) = h_L$

So, such conditions appears as  $h_{mean}(0) = h_0$  and  $h_{mean}(L) = h_L$  in the steady part and as  $\bar{h}(0, \omega) = \bar{h}(L, \omega) = 0$  in the transient part. Thus, the analytical solution for this model can be obtained, it appears that this solution does not depend on the model width  $W$ :

$$h(x, t) = \frac{R_{mean}}{2T}(Lx - x^2) + \frac{h_L - h_0}{L}x + h_0 + \sum Re\{e^{i\omega t} \left[ \bar{R} \frac{X^2}{T} \left( 1 + \frac{\sinh \frac{x-L}{X} - \sinh \frac{x}{X}}{\sinh \frac{L}{X}} \right) \right]\} \quad (A9)$$



### A3 Analytical inversion: solution to determine the recharge rate $R(t)$

Analytical solutions presented previously constitutes a computationally much faster method than numerical models to represent hydraulic heads. They also offer the possibility to recompute analytically recharge rate  $R(t)$  from hydraulic head variations  
620  $h(x, t)$ .

As developed before, we will separate the steady state and the transient state. Focusing on the transient terms from equations A8 and A9, respectively for the "pumping" and "natural" case, we obtain:

$$\bar{R}(\omega) = \left( i\omega S\bar{h}(x, \omega) - \frac{\bar{Q}}{XW} \frac{\sinh \frac{x-L}{X}}{\cosh \frac{L}{X}} \right) \times \left( 1 - \frac{\cosh \frac{x}{X}}{\cosh \frac{L}{X}} \right)^{-1} \quad (\text{A10})$$

$$625 \quad \bar{R}(\omega) = i\omega S\bar{h}(x, \omega) \left( 1 + \frac{\sinh \frac{x-L}{X} - \sinh \frac{x}{X}}{\sinh \frac{L}{X}} \right)^{-1} \quad (\text{A11})$$

Then, time domain recharge fluctuations (RF) are computed by inverse Fourier transform of  $\bar{R}(\omega)$  (Eq. A2). As only the transient state is developed here, RF are equal to recharge rate variations minus the mean recharge rate along the studied period.

### Appendix B: Validation of the analytical model

630 Following Cuthbert (2010), we tested our method with a virtual case using a ModFlow numerical model. This model is composed of one row and 200 columns with a mesh size of 10 m to obtain a 1D geometry. We simulate a confined layer of transmissivity  $T = 1 \times 10^{-3} \text{ m}^2 \cdot \text{s}^{-1}$  and of storage coefficient  $S = 0.05$ . Heads are imposed at  $x = 0$  and  $x = 2000 \text{ m}$ . By construction, the 1D numerical model is equivalent to the 1D analytical model used for the Guidel site (natural case).

#### B1 Simulating water table fluctuations from recharge fluctuations

635 GW level fluctuations from the analytical and numerical models are compared. The imposed recharge was computed from the Thornthwaite soil model. To mimic the steady state of the analytical model, the initial condition in the numerical model is defined by applying mean recharge rate. As illustrated on figure B1, both analytical and numerical solutions fit well. One main difference appears the first two years because the analytical model does not consider any initial state. Indeed, the numerical model underestimates GW levels at the beginning of the simulation because the steady-state GW levels were used as initial  
640 state while the simulation starts in January, during the humid period.

#### B2 Accuracy of recharge inversion

In a second time, we performed a numerical test to estimate the ability of the analytic approach to estimate RF. This experience is based on a comparison with the ModFlow model described previously. At the end of the numerical simulation, hydraulic

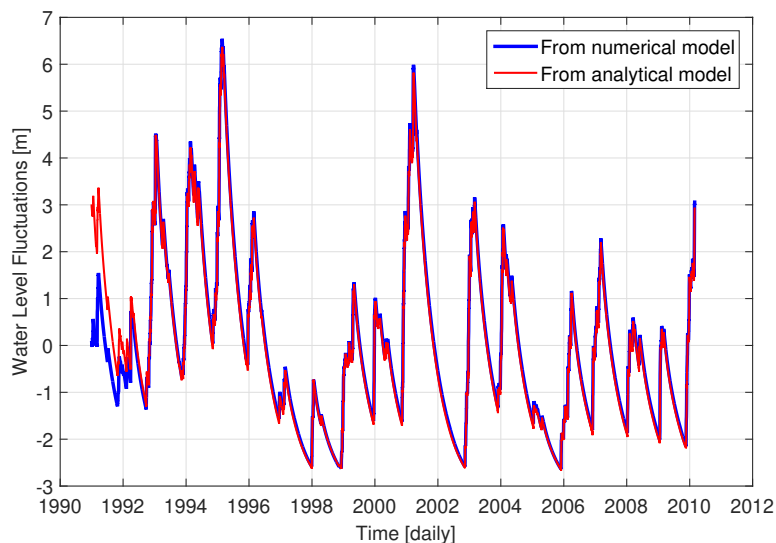


**Figure B1.** Comparison of water table fluctuations, at  $x = 1500m$ , obtained from analytical and numerical models. Note that the steady-state term (the mean value) has been removed.

head at  $x = 1500 m$  is recorded (blue curve on Fig. B1) and will be used to recover RF analytically (Eq. A11). Then, this  
645 inverted RF will be compared to the RF imposed to the ModFlow model. We tried to answer to two questions, namely (1) at  
which time scale is recharge well estimated? and (2) what is the impact of parameter uncertainties on RF estimates?

Although the analytical model can be run at the same time step than the well data, RF estimates are affected by (1) numerical  
oscillations linked to the discrete frequency-domain computations over a finite length time series and (2) the amplification of  
high-frequency GW head variations, including observation errors. Estimated RF can be integrated over time to avoid these  
650 spurious oscillations. Overall, an integration time larger than a few original time steps is sufficient to ensure an estimation of  
the recharged volume at a 99% level (Fig. B2). An accurate recovery of temporal variations, though, requires integration over  
10 time steps to reach determination and correlation coefficients  $r, r^2 > 0.95$ .

This test gives also an idea of parameters uncertainties. We can see how RF estimated from GW levels are influenced in terms  
of timing and mean amplitude. Parameters ( $T$ ,  $S$  and  $L$ ) uncertainty has logically an important impact. However, uncertainty  
655 on characteristic time has a limited impact on both timing and amplitude of RF as shown on figure B3.

### Appendix C: Mean groundwater level and mean recharge estimates

We explored the stationary part of equation A8 (pumping case), defining the relationships between aquifer transmissivity, long-  
term mean recharge and flow. In theory, and in homogeneous media,  $R_{mean}/T$  can be directly estimated from the quadratic  
shape of the water table (Eq. A8), i.e. the deviation of mean GW level with respect to a linear evolution. On Figure C1, mean

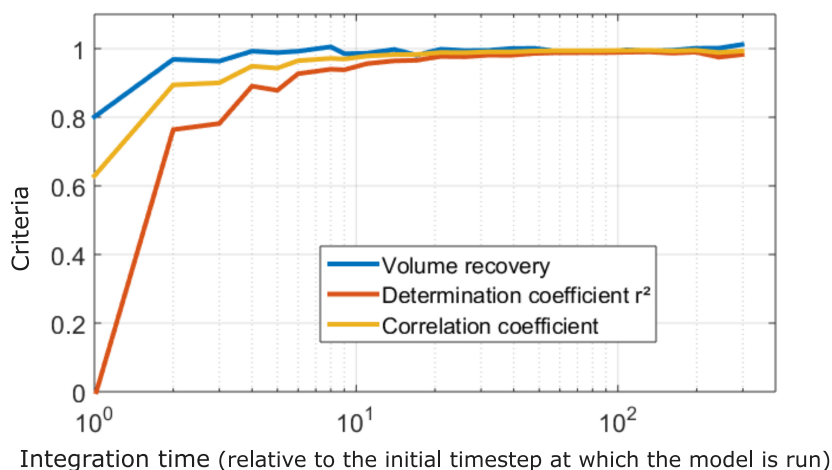


**Figure B2.** Impact of integration time on recharge volume and determination coefficient  $r^2$ . Here, "volume recovery" refers to the ratio between inferred and true (initially imposed to the numerical ModFlow model) mean annual amplitude.

660 GW levels observed in Ploemeur are projected along the  $x$  axis and are compared to one of the best steady-state model. Note that on Figure C1, modeled mean GW level has a quadratic component while it appears mostly linear. In spite of this apparent good restitution of mean GW levels, equifinality on parameters ( $R_{mean}$ ,  $T$ ,  $L$  and  $h_L$ ) occurs. It is clear that heterogeneity affects deeply mean GW levels, so that separating the impact of recharge and heterogeneity on mean GW level is difficult.

In addition, we investigated this steady-state issue using a numerical homogeneous 2D MODFLOW model. The actual 10m-  
665 resolution topography was imposed as upper boundary conditions (DRAIN PACKAGE) and pumping wells were set up at their actual position in the domain with their respective pumping rates. The advantage of such model was to set a realistic geometry and to remove "geometric" parameters like model length  $L$  and imposed head  $h_L$  (steady-state term of Eq. A8). So, we kept only two parameters in this calibration: mean recharge rate ( $R_{mean}$ ) and transmissivity ( $T$ ). Results showed that  $T$  and  $R_{mean}/T$  ratio seems well constrained when focusing on mean water levels measured in several boreholes. However,  $T$  and  
670  $R_{mean}/T$  estimates are not relevant because they are sensitive to the boreholes selected for the calibration and to the presence of potential heterogeneities.

Finally, the information content of mean GW levels is limited by (1) incomplete sampling within the observation network, considering the punctual nature of borehole data with respect to local heterogeneities in recharge and hydrodynamic properties, blurring the evolution of hydraulic head in space (Fig. C1); (2) incomplete sampling of the GW system as the observation  
675 network represents only a limited part of the aquifer; and (3) limitations linked to hypotheses in the conceptual model. Uncertainties in actual boundary conditions, such as the representation of local GW behavior close to the pumping wells also limit interpretation. The inability to constrain transmissivity and mean recharge from long-term mean well observations is in line with several studies (e.g. Sánchez-Vila et al., 1996).

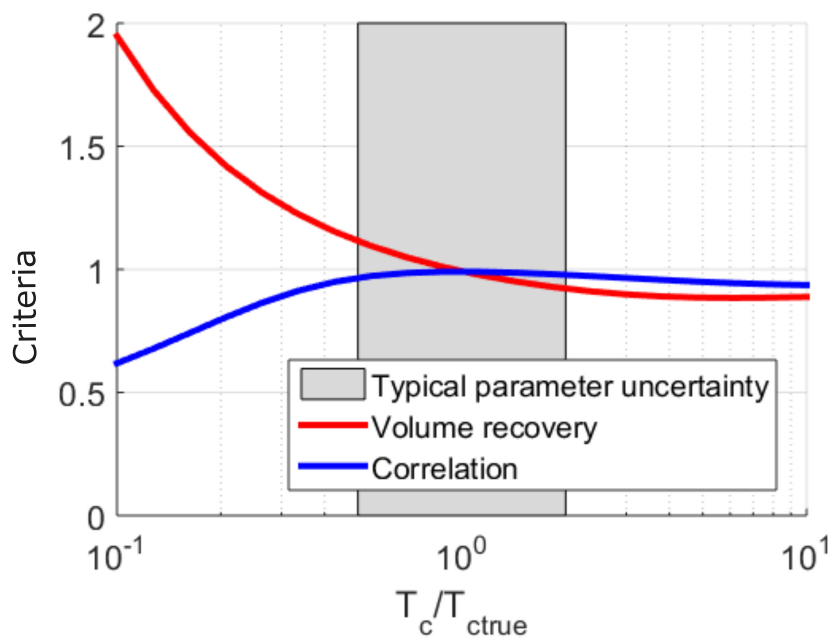


**Figure B3.** Impact of uncertainties on the estimation of characteristic time  $t_c$  on recharge amplitude and timing recovery. The gray rectangle defines the typical uncertainty on estimated characteristic time. Here, "volume recovery" refers to the ratio between inferred and true mean annual amplitude

*Author contributions.* Data collection and pre-processing: NL and LG. Models development: LG and LL. Simulations: LG. Post-processing  
680 of the simulated data: LG and LL. Results interpretation: LG, LL, OB and JM. LG prepared the manuscript with contributions from LL, OB  
and JM

*Competing interests.* Authors declare no competing interests.

*Acknowledgements.* This work is part of the ANR project EQUIPEX CRITEX (grant ANR-11-EQPX-0011) and set on the Ploemeur Critical  
685 Zone Observatory  $H^+$  (SNO H+, <http://hplus.ore.fr/en/ploemeur>). We are grateful to the OZCAR research infrastructure (<http://www.ozcar-ri.org/>). We thank M. Smilovic for revising the manuscript for grammar and syntax.

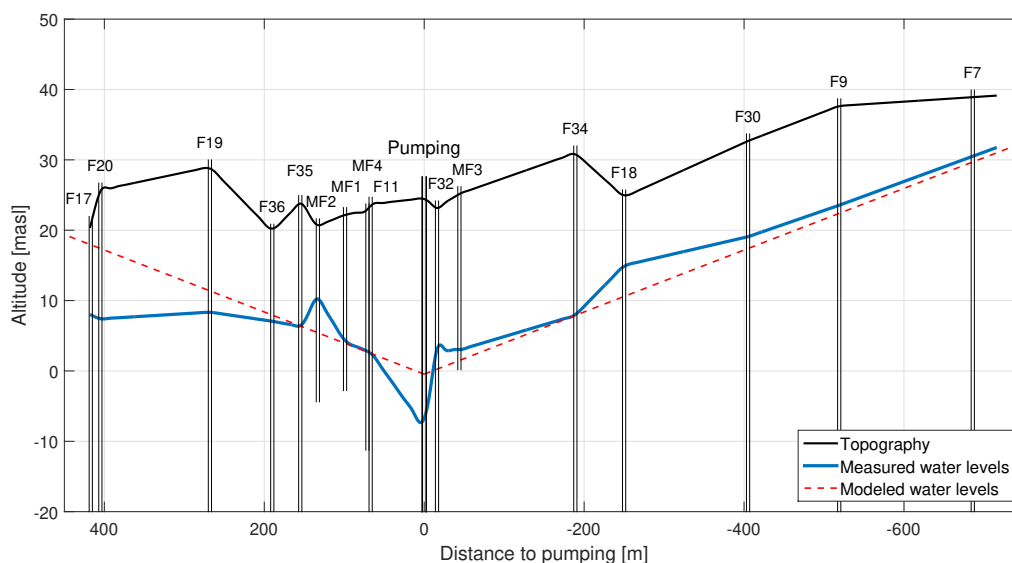


**Figure C1.** Mean GW levels observed on the Ploemeur site (blue curve), shown on a SE-NW cross section. The red dashed curve represents the best 1D steady-state analytical model which has the lowest least square difference between data and model.

## References

- Ajami, H., Sharma, A., Band, L. E., Evans, J. P., Tuteja, N. K., Amirthanathan, G. E., and Bari, M. A.: On the non-stationarity of hydrological response in anthropogenically unaffected catchments: An Australian perspective, *Hydrology and Earth System Sciences*, 21, 281–294, <https://doi.org/10.5194/hess-21-281-2017>, 2017.
- 690 Alley, W. M., Healy, R. W., LaBaugh, J. W., and Reilly, T. E.: Flow and storage in groundwater systems, <https://doi.org/10.1126/science.1067123>, 2002.
- Appels, W. M., Graham, C. B., Freer, J. E., and McDonnell, J. J.: Factors affecting the spatial pattern of bedrock groundwater recharge at the hillslope scale, *Hydrological Processes*, 29, 4594–4610, <https://doi.org/10.1002/hyp.10481>, 2015.
- Barron, O. V., Crosbie, R. S., Dawes, W. R., Charles, S. P., Pickett, T., and Donn, M. J.: Climatic controls on diffuse groundwater recharge  
695 across Australia, *Hydrology and Earth System Sciences*, 16, 4557–4570, <https://doi.org/10.5194/hess-16-4557-2012>, 2012.
- Bense, V. F., Gleeson, T., Loveless, S. E., Bour, O., and Scibek, J.: Fault zone hydrogeology, *Earth-Science Reviews*, 127, 171–192, <https://doi.org/10.1016/j.earscirev.2013.09.008>, 2013.
- Besbes, M. and Marsily, G. D. E.: From infiltration to recharge: use of a parametric transfer function, *Journal of Hydrology*, 74, 271–293, 1984.
- 700 Blöschl, G., Bierkens, M. F., Chambel, A., Cudennec, C., Destouni, G., Fiori, A., Kirchner, J. W., McDonnell, J. J., Savenije, H. H., Sivapalan, M., Stumpp, C., Toth, E., Volpi, E., and Carr, G.: Twenty-three unsolved problems in hydrology (UPH)—a community perspective, *Hydrological Sciences Journal*, 64, 1141–1158, <https://doi.org/10.1080/02626667.2019.1620507>, 2019.



- Bochet, O., Bethencourt, L., Dufresne, A., Farasin, J., Pédrot, M., Labasque, T., Chatton, E., Lavenant, N., Petton, C., Abbott, B. W., Aquilina, L., and Le Borgne, T.: Iron-oxidizer hotspots formed by intermittent oxic–anoxic fluid mixing in fractured rocks, *Nature Geoscience*, 13, 705 <https://doi.org/10.1038/s41561-019-0509-1>, 2020.
- Bredehoeft, J.: The water budget myth Revisited: Why Hydrogeologists Model, <https://doi.org/10.1111/j.1745-6584.2002.tb02511.x>, 2002.
- Bresciani, E., Goderniaux, P., and Batelaan, O.: Hydrogeological controls of water table - land surface interactions, *Geophysical Research Letters*, pp. 1–9, <https://doi.org/10.1002/2016GL070618>, 2016.
- Cao, G., Scanlon, B. R., Han, D., and Zheng, C.: Impacts of thickening unsaturated zone on groundwater recharge in the North China Plain, *Journal of Hydrology*, 537, 260–270, <https://doi.org/10.1016/j.jhydrol.2016.03.049>, 2016.
- 710 Carslaw, H. S. and Jaeger, J. C.: *Conduction of heat in solids*: Oxford Science Publications, Oxford, England, 1959.
- Clark, M. P., Bierkens, M. F., Samaniego, L., Woods, R. A., Uijlenhoet, R., Bennett, K. E., Pauwels, V. R., Cai, X., Wood, A. W., and Peters-Lidard, C. D.: The evolution of process-based hydrologic models: Historical challenges and the collective quest for physical realism, *Hydrology and Earth System Sciences*, 21, 3427–3440, <https://doi.org/10.5194/hess-21-3427-2017>, 2017.
- 715 Clauser, C.: Permeability of crystalline rocks, *Eos, Transactions American Geophysical Union*, 73, 233–238, 1992.
- Collenteur, R. A., Bakker, M., Klammler, G., and Birk, S.: Estimation of groundwater recharge from groundwater levels using non-linear transfer function noise models and comparison to lysimeter data, *Hydrology and Earth System Sciences*, 25, 2931–2949, <https://doi.org/10.5194/hess-25-2931-2021>, 2021.
- Condon, L. E. and Maxwell, R. M.: Systematic shifts in Budyko relationships caused by groundwater storage changes, *Hydrology and Earth System Sciences*, 21, 1117–1135, <https://doi.org/10.5194/hess-21-1117-2017>, 2017.
- 720 Crosbie, R. S., Binning, P., and Kalma, J. D.: A time series approach to inferring groundwater recharge using the water table fluctuation method, *Water Resources Research*, 41, 1–9, <https://doi.org/10.1029/2004WR003077>, 2005.
- Cuthbert, M. O.: An improved time series approach for estimating groundwater recharge from groundwater level fluctuations, *Water Resources Research*, 46, 1–11, <https://doi.org/10.1029/2009WR008572>, 2010.
- 725 Cuthbert, M. O., Acworth, R., Andersen, M. S., Larsen, J. R., McCallum, A. M., Rau, G. C., and Tellam, J. H.: Understanding and quantifying focused, indirect groundwater recharge from ephemeral streams using water table fluctuations, *Water Resources Research*, 52, 827–850, <https://doi.org/10.1002/2015WR017503>, 2016.
- Cuthbert, M. O., Gleeson, T., Moosdorf, N., Befus, K. M., Schneider, A., Hartmann, J., and Lehner, B.: Global patterns and dynamics of climate–groundwater interactions, *Nature Climate Change*, 9, 137–141, <https://doi.org/10.1038/s41558-018-0386-4>, 2019a.
- 730 Cuthbert, M. O., Taylor, R. G., Favreau, G., Todd, M. C., Shamsudduha, M., Villholth, K. G., MacDonald, A. M., Scanlon, B. R., Kotchoni, D. O., Vouillamoz, J. M., Lawson, F. M., Adjomayi, P. A., Kashaigili, J., Seddon, D., Sorensen, J. P., Ebrahim, G. Y., Owor, M., Nyenje, P. M., Nazoumou, Y., Goni, I., Ousmane, B. I., Sibanda, T., Ascott, M. J., Macdonald, D. M., Agyekum, W., Koussoubé, Y., Wanke, H., Kim, H., Wada, Y., Lo, M. H., Oki, T., and Kukuric, N.: Observed controls on resilience of groundwater to climate variability in sub-Saharan Africa, *Nature*, 572, 230–234, <https://doi.org/10.1038/s41586-019-1441-7>, 2019b.
- 735 Dalin, C., Wada, Y., Kastner, T., and Puma, M. J.: Groundwater depletion embedded in international food trade, *Nature*, 543, 700–704, <https://doi.org/10.1038/nature21403>, 2017.
- De Marsily, G.: *Quantitative hydrogeology*, Academic Press, 1986.
- de Vries, J. J. and Simmers, I.: Groundwater recharge: An overview of process and challenges, *Hydrogeology Journal*, 10, 5–17, <https://doi.org/10.1007/s10040-001-0171-7>, 2002.





- 740 Dewandel, B., Aunay, B., Maréchal, J. C., Roques, C., Bour, O., Mougin, B., and Aquilina, L.: Analytical solutions for analysing pumping tests in a sub-vertical and anisotropic fault zone draining shallow aquifers, *Journal of Hydrology*, 509, 115–131, <https://doi.org/10.1016/j.jhydrol.2013.11.014>, 2014.
- Dickinson, J. E.: Inferring time-varying recharge from inverse analysis of long-term water levels, *Water Resources Research*, 40, 1–15, <https://doi.org/10.1029/2003WR002650>, 2004.
- 745 Döll, P. and Fiedler, K.: Global-scale modeling of groundwater recharge, *Hydrology and Earth System Sciences*, 12, 863–885, <https://doi.org/10.5194/hess-12-863-2008>, 2008.
- Domenico, P. A. and Schwartz, F. W.: *Physical and chemical hydrogeology*. Second edition, Wiley, 1998.
- Earle, S.: *Physical geology*, <https://doi.org/10.1016/B978-0-444-42758-8.50008-8>, 2015.
- Fan, Y.: Groundwater in the Earth’s critical zone: Relevance to large-scale patterns and processes, *Water Resources Research*, 51, 3052–3069, <https://doi.org/10.1002/2015WR017037>, 2015.
- 750 Fan, Y., Clark, M., Lawrence, D. M., Swenson, S., Band, L. E., Brantley, S. L., Brooks, P. D., Dietrich, W. E., Flores, A., Grant, G., Kirchner, J. W., Mackay, D. S., McDonnell, J. J., Milly, P. C., Sullivan, P. L., Tague, C., Ajami, H., Chaney, N., Hartmann, A., Hazenberg, P., McNamara, J., Pelletier, J., Perket, J., Rouholahnejad-Freund, E., Wagener, T., Zeng, X., Beighley, E., Buzan, J., Huang, M., Livneh, B., Mohanty, B. P., Nijssen, B., Safeeq, M., Shen, C., van Verseveld, W., Volk, J., and Yamazaki, D.: Hillslope Hydrology in Global Change Research and Earth System Modeling, *Water Resources Research*, pp. 1737–1772, <https://doi.org/10.1029/2018WR023903>, 2019.
- 755 Favreau, G., Cappelaere, B., Massuel, S., Leblanc, M., Boucher, M., Boulain, N., and Leduc, C.: Land clearing, climate variability, and water resources increase in semiarid southwest Niger: A review, *Water Resources Research*, 45, 1–18, <https://doi.org/10.1029/2007WR006785>, 2009.
- Gabrielli, C. P. and McDonnell, J. J.: No Direct Linkage Between Event-Based Runoff Generation and Groundwater Recharge on the Maimai Hillslope, *Water Resources Research*, 54, 8718–8733, <https://doi.org/10.1029/2017WR021831>, 2018.
- 760 Gaillardet, J., Braud, I., Hankard, F., Anquetin, S., Bour, O., Dorfliger, N., Dreuzy, J. d., Galle, S., Galy, C., Gogo, S., Gourcy, L., Habets, F., Laggoun, F., Longuevergne, L., and Borgne, T. L.: OZCAR : The French Network of Critical Zone Observatories, *Vadose Zone Journal*, 17, <https://doi.org/10.2136/vzj2018.04.0067>, 2018.
- Gauvain, A., Leray, S., Marçais, J., Roques, C., Vautier, C., Gresselin, F., Aquilina, L., and de Dreuzy, J. R.: Geomorphological Controls on Groundwater Transit Times: A Synthetic Analysis at the Hillslope Scale, *Water Resources Research*, 57, <https://doi.org/10.1029/2020WR029463>, 2021.
- 765 Gee, G. W. and Hillel, D.: Groundwater recharge in arid regions: Review and critique of estimation methods, *Hydrological Processes*, 2, 255–266, <https://doi.org/10.1002/hyp.3360020306>, 1988.
- Gelhar, L. W.: Stochastic analysis of phreatic aquifers, *Water Resources Research*, 10, 539–545, <https://doi.org/10.1029/WR010i003p00539>, 1974.
- 770 Gerten, D., Lucht, W., Ostberg, S., Heinke, J., Kowarsch, M., Kreft, H., Kundzewicz, Z. W., Rastgooy, J., Warren, R., and Schellhuber, H. J.: Asynchronous exposure to global warming: Freshwater resources and terrestrial ecosystems, *Environmental Research Letters*, 8, <https://doi.org/10.1088/1748-9326/8/3/034032>, 2013.
- Gleeson, T., Wada, Y., Bierkens, M. F. P., and van Beek, L. P. H.: Water balance of global aquifers revealed by groundwater footprint, *Nature*, 488, 197–200, <https://doi.org/10.1038/nature11295>, 2012.
- 775



- Guihéneuf, N., Boisson, A., Bour, O., Dewandel, B., Perrin, J., Dausse, A., Viossanges, M., Chandra, S., Ahmed, S., and Maréchal, J. C.: Groundwater flows in weathered crystalline rocks: Impact of piezometric variations and depth-dependent fracture connectivity, *Journal of Hydrology*, 511, 320–324, <https://doi.org/10.1016/j.jhydrol.2014.01.061>, 2014.
- 780 Guillaumot, L., Marçais, J., Vautier, C., Guillou, A., Vergnaud, V., Bouchez, C., Dupas, R., Durand, P., Dreuzy, J.-r. D., and Aquilina, L.: A hillslope-scale aquifer-model to determine past agricultural legacy and future nitrate concentrations in rivers, *Science of the Total Environment*, 800, 149 216, <https://doi.org/10.1016/j.scitotenv.2021.149216>, 2021.
- Hartmann, A., Gleeson, T., Wada, Y., and Wagener, T.: Enhanced groundwater recharge rates and altered recharge sensitivity to climate variability through subsurface heterogeneity, *Proceedings of the National Academy of Sciences*, 114, 2842–2847, <https://doi.org/10.1073/pnas.1614941114>, 2017.
- 785 Healy, R. W.: *Estimating groundwater recharge*, Cambridge University Press, 2010.
- Healy, R. W. and Cook, P. G.: Using groundwater levels to estimate recharge, *Hydrogeology Journal*, 10, 91–109, <https://doi.org/10.1007/s10040-001-0178-0>, 2002.
- Hector, B., Cohard, J.-m., Séguis, L., Galle, S., and Peugeot, C.: Hydrological functioning of West-African inland valleys explored with a critical zone model, *Hydrology and Earth System Sciences Discussions*, 22, 1–35, 2018.
- 790 Herzog, A., Hector, B., Cohard, J. M., Vouillamoz, J. M., Lawson, F. M. A., Peugeot, C., and de Graaf, I.: A parametric sensitivity analysis for prioritizing regolith knowledge needs for modeling water transfers in the West African critical zone, *Vadose Zone Journal*, 20, 1–22, <https://doi.org/10.1002/vzj2.20163>, 2021.
- Hill, M. C.: The practical use of simplicity in developing ground water models, *Ground Water*, 44, 775–781, <https://doi.org/10.1111/j.1745-6584.2006.00227.x>, 2006.
- 795 Hiscock, K.: *Hydrogeology: Principles and Practice.*, <https://doi.org/10.1007/s12665-016-5360-8>, 2009.
- Jasechko, S., Birks, S. J., Gleeson, T., Wada, Y., Fawcett, P. J., Sharp, Z. D., McDonnell, J. J., and Welker, J. M.: The pronounced seasonality of global groundwater recharge, *Water Resources Research*, 50, 8845–8867, <https://doi.org/10.1002/2014WR015809>.Received, 2014.
- Jimenez-Martinez, J., Longuevergne, L., Le Borgne, T., Davy, P., Russian, A., and Bour, O.: Temporal and spatial scaling of hydraulic response to recharge in fractured aquifers: Insights from a frequency domain analysis, *Water Resources Research*, 49, 3007–3023, <https://doi.org/10.1002/wrcr.20260>, 2013.
- 800 Johansen, O. M., Pedersen, M. L., and Jensen, J. B.: Effect of groundwater abstraction on fen ecosystems, *Journal of Hydrology*, 402, 357–366, <https://doi.org/10.1016/j.jhydrol.2011.03.031>, 2011.
- Kendy, E., Zhang, Y., Liu, C., Wang, J., and Steenhuis, T.: Groundwater recharge from irrigated cropland in the North China Plain: Case study of Luancheng County, Hebei Province, 1949-2000, *Hydrological Processes*, <https://doi.org/10.1002/hyp.5529>, 2004.
- 805 Kollet, S. J.: Influence of soil heterogeneity on evapotranspiration under shallow water table conditions: Transient, stochastic simulations, *Environmental Research Letters*, 4, <https://doi.org/10.1088/1748-9326/4/3/035007>, 2009.
- Kollet, S. J. and Maxwell, R. M.: Capturing the influence of groundwater dynamics on land surface processes using an integrated, distributed watershed model, *Water Resources Research*, 44, 1–18, <https://doi.org/10.1029/2007WR006004>, 2008.
- Kovacs, G.: *Seepage hydraulics.*, Elsevier, [https://doi.org/10.1016/0022-1694\(84\)90254-3](https://doi.org/10.1016/0022-1694(84)90254-3), 1981.
- 810 Labrecque, G., Chesnaux, R., and Boucher, M.-a.: Water-table fluctuation method for assessing aquifer recharge : application to Canadian aquifers and comparison with other methods, pp. 521–533, 2020.



- Lague, D., Davy, P., and Crave, A.: Estimating Uplift Rate and Erodibility from the Area-Slope Relationship : Examples from Brittany ( France ) and Numerical Modelling, *Physics and Chemistry of the Earth Part A Solid Earth and Geodesy*, 25, 543–548, [https://doi.org/10.1016/S1464-1895\(00\)00083-1](https://doi.org/10.1016/S1464-1895(00)00083-1), 2000.
- 815 Le Borgne, T., Bour, O., Paillet, F. L., and Caudal, J. P.: Assessment of preferential flow path connectivity and hydraulic properties at single-borehole and cross-borehole scales in a fractured aquifer, *Journal of Hydrology*, 328, 347–359, <https://doi.org/10.1016/j.jhydrol.2005.12.029>, 2006.
- Le Borgne, T., Bour, O., Riley, M. S., Gouze, P., Pezard, P. A., Belghoul, A., Lods, G., Le Provost, R., Greswell, R. B., Ellis, P. A., Isakov, E., and Last, B. J.: Comparison of alternative methodologies for identifying and characterizing preferential flow paths in heterogeneous  
820 aquifers, *Journal of Hydrology*, 345, 134–148, <https://doi.org/10.1016/j.jhydrol.2007.07.007>, 2007.
- Le Coz, M., Favreau, G., and Ousmane, S. D.: Modeling Increased Groundwater Recharge due to Change from Rainfed to Irrigated Cropping in a Semiarid Region, *Vadose Zone Journal*, 12, vzj2012.0148, <https://doi.org/10.2136/vzj2012.0148>, 2013.
- Lee, L. J. E., Lawrence, D. S. L., and Price, M.: Analysis of water-level response to rainfall and implications for recharge pathways in the Chalk aquifer, SE England, *Journal of Hydrology*, 330, 604–620, <https://doi.org/10.1016/j.jhydrol.2006.04.025>, 2006.
- 825 Leray, S., de Dreuzy, J. R., Bour, O., Labasque, T., and Aquilina, L.: Contribution of age data to the characterization of complex aquifers, *Journal of Hydrology*, 464–465, 54–68, <https://doi.org/10.1016/j.jhydrol.2012.06.052>, 2012.
- Leray, S., de Dreuzy, J. R., Aquilina, L., Vergnaud-Ayraud, V., Labasque, T., Bour, O., and Le Borgne, T.: Temporal evolution of age data under transient pumping conditions, *Journal of Hydrology*, 511, 555–566, <https://doi.org/10.1016/j.jhydrol.2014.01.064>, 2014.
- Liu, R., Li, B., Jiang, Y., and Huang, N.: Review: Mathematical expressions for estimating equivalent permeability of rock fracture networks,  
830 *Hydrogeology Journal*, <https://doi.org/10.1007/s10040-016-1441-8>, 2016.
- Long, D., Longuevergne, L., and Scanlon, B. R.: Uncertainty in evapotranspiration fromland surfacemodeling, remote sensing, and GRACE satellites, *Water Resources Research*, 50, 1131–1151, <https://doi.org/10.1002/2013WR014581>.Received, 2014.
- MacDonald, A. M. and Calow, R. C.: Developing groundwater for secure rural water supplies in Africa, *Desalination*, 248, 546–556, <https://doi.org/10.1016/j.desal.2008.05.100>, 2009.
- 835 Marçais, J., de Dreuzy, J. R., and Erhel, J.: Dynamic coupling of subsurface and seepage flows solved within a regularized partition formulation, *Advances in Water Resources*, 109, 94–105, <https://doi.org/10.1016/j.advwatres.2017.09.008>, 2017.
- Maréchal, J. C., Dewandel, B., Ahmed, S., Galeazzi, L., and Zaidi, F. K.: Combined estimation of specific yield and natural recharge in a semi-arid groundwater basin with irrigated agriculture, *Journal of Hydrology*, 329, 281–293, <https://doi.org/10.1016/j.jhydrol.2006.02.022>, 2006.
- 840 Martin, C., Molénat, J., Gascuel-Oudou, C., Vouillamoz, J. M., Robain, H., Ruiz, L., Faucheux, M., and Aquilina, L.: Modelling the effect of physical and chemical characteristics of shallow aquifers on water and nitrate transport in small agricultural catchments, *Journal of Hydrology*, 326, 25–42, <https://doi.org/10.1016/j.jhydrol.2005.10.040>, 2006.
- Masson, V., Le Moigne, P., Martin, E., Faroux, S., Alias, A., Alkama, R., Belamari, S., Barbu, A., Boone, A., Bouyssel, F., Brousseau, P., Brun, E., Calvet, J. C., Carrer, D., Decharme, B., Delire, C., Donier, S., Essaouini, K., Gibelin, A. L., Giordani, H., Habets, F., Jidane, M.,  
845 Kerdraon, G., Kourzeneva, E., Lafaysse, M., Lafont, S., Lebeau-pin Brossier, C., Lemonsu, A., Mahfouf, J. F., Marguinaud, P., Mokhtari, M., Morin, S., Pigeon, G., Salgado, R., Seity, Y., Taillefer, F., Tanguy, G., Tulet, P., Vincendon, B., Vionnet, V., and Voltaire, A.: The SURFEXv7.2 land and ocean surface platform for coupled or offline simulation of earth surface variables and fluxes, *Geoscientific Model Development*, 6, 929–960, <https://doi.org/10.5194/gmd-6-929-2013>, 2013.



- Maxwell, R. M. and Condon, L. E.: Connections between groundwater flow and transpiration partitioning, *Science*, 353, 377–380,  
850 <https://doi.org/10.1126/science.aaf7891>, 2016.
- Meier, P. M., Carrera, J., and Sánchez-Vila, X.: An evaluation of Jacob’s method for the interpretation of pumping tests in heterogeneous  
formations, *Water Resources Research*, 34, 1011–1025, <https://doi.org/10.1029/98WR00008>, 1998.
- Mileham, L., Taylor, R. G., Todd, M., Tindimugaya, C., and Thompson, J.: The impact of climate change on groundwater recharge and  
runoff in a humid, equatorial catchment: sensitivity of projections to rainfall intensity, *Hydrological Sciences Journal*, 54, 727–738,  
855 <https://doi.org/10.1623/hysj.54.4.727>, 2009.
- Mohan, C., Western, A. W., Wei, Y., and Saft, M.: Predicting groundwater recharge for varying landcover and climate conditions: a global  
meta-study, *Hydrology and Earth System Sciences Discussions*, 22, 1–22, <https://doi.org/10.5194/hess-2017-679>, 2017.
- Molénat, J., Davy, P., Gascuel-Oudou, C., and Durand, P.: Study of three subsurface hydrologic systems based on spectral and cross-spectral  
analysis of time series, *Journal of Hydrology*, 222, 152–164, [https://doi.org/10.1016/S0022-1694\(99\)00107-9](https://doi.org/10.1016/S0022-1694(99)00107-9), 1999.
- 860 Morton, F. I.: Operational estimates of areal evapotranspiration and their significance to the science and practice of hydrology, *Journal of*  
*Hydrology*, 66, 1–76, [https://doi.org/10.1016/0022-1694\(83\)90177-4](https://doi.org/10.1016/0022-1694(83)90177-4), 1983.
- Nicolas, M., Bour, O., Selles, A., Dewandel, B., Bailly-comte, V., Chandra, S., Ahmed, S., and Maréchal, J.-c.: Managed Aquifer Recharge  
in fractured crystalline rock aquifers : Impact of horizontal preferential flow on recharge dynamics, *Journal of Hydrology*, 573, 717–732,  
<https://doi.org/10.1016/j.jhydrol.2019.04.003>, 2019.
- 865 Noilhan, J. and Planton, S.: A Simple Parameterization of Land Surface Processes for Meteorological Models, [https://doi.org/10.1175/1520-0493\(1989\)117<0536:ASPOLS>2.0.CO;2](https://doi.org/10.1175/1520-0493(1989)117<0536:ASPOLS>2.0.CO;2), 1989.
- Owor, M., Taylor, R., Tindimugaya, C., and Mwesigwa, D.: Rainfall intensity and groundwater recharge: empirical evidence from the Upper  
Nile Basin, *Environmental Research Letters*, 4, 1–6, <https://doi.org/10.1088/1748-9326/4/3/035009>, 2009.
- Perkins, K. S., Nimmo, J. R., Medeiros, A. C., Szutu, D. J., and von Allmen, E.: Assessing effects of native forest restoration on soil moisture  
870 dynamics and potential aquifer recharge, *Auwahi, Maui, Ecohydrology*, 7, 1437–1451, <https://doi.org/10.1002/eco.1469>, 2014.
- Perrin, C., Michel, C., and Andréassian, V.: Improvement of a parsimonious model for streamflow simulation, *Journal of Hydrology*, 279,  
275–289, [https://doi.org/10.1016/S0022-1694\(03\)00225-7](https://doi.org/10.1016/S0022-1694(03)00225-7), 2003.
- Pouladi, B., Bour, O., Longuevergne, L., de La Bernardie, J., and Simon, N.: Modelling borehole flows from Distributed Temperature Sensing  
data to monitor groundwater dynamics in fractured media, *Journal of Hydrology*, 598, <https://doi.org/10.1016/j.jhydrol.2021.126450>,  
875 2021.
- Riedel, T. and Weber, T. K. D.: Review: The influence of global change on Europe’s water cycle and groundwater recharge, *Hydrogeology*  
*Journal*, 28, 1939–1959, <https://doi.org/10.1007/s10040-020-02165-3>, 2020.
- Roques, C., Bour, O., Aquilina, L., and Dewandel, B.: High yielding aquifers in crystalline basement: insights about the role of fault zones,  
exemplified by Armorican Massif, France, *Hydrogeology Journal*, pp. 1–14, <https://doi.org/10.1007/s10040-016-1451-6>, 2016.
- 880 Roques, C., Aquilina, L., Boisson, A., Vergnaud-Ayraud, V., Labasque, T., Longuevergne, L., Laurencelle, M., Dufresne, A.,  
de Dreuzy, J. R., Pauwels, H., and Bour, O.: Autotrophic denitrification supported by biotite dissolution in crystalline aquifers:  
(2) transient mixing and denitrification dynamic during long-term pumping, *Science of the Total Environment*, 619-620, 491–503,  
<https://doi.org/10.1016/j.scitotenv.2017.11.104>, 2018.
- Rousseau-Gueutin, P., Love, A. J., Vasseur, G., Robinson, N. I., Simmons, C. T., and De Marsily, G.: Time to reach near-steady state in large  
885 aquifers, *Water Resources Research*, 49, 6893–6908, <https://doi.org/10.1002/wrcr.20534>, 2013.



- Rovey, C. W. and Cherkauer, D. S.: Scale Dependency of Hydraulic Conductivity Measurements, <https://doi.org/10.1111/j.1745-6584.1995.tb00023.x>, 1995.
- Ruelleu, S., Moreau, F., Bour, O., Gapais, D., and Martelet, G.: Impact of gently dipping discontinuities on basement aquifer recharge: An example from Ploemeur (Brittany, France), *Journal of Applied Geophysics*, 70, 161–168, <https://doi.org/10.1016/j.jappgeo.2009.12.007>, 2010.
- Sánchez-Vila, X., Carrera, J., and Girardi, J. P.: Scale effects in transmissivity, *Journal of Hydrology*, 183, 1–22, [https://doi.org/10.1016/S0022-1694\(96\)80031-X](https://doi.org/10.1016/S0022-1694(96)80031-X), 1996.
- Scanlon, B. R., Healy, R. W., and Cook, P. G.: Choosing appropriate technique for quantifying groundwater recharge, *Hydrogeology Journal*, 10, 18–39, <https://doi.org/10.1007/s10040-0010176-2>, 2002.
- 895 Scanlon, B. R., Keese, K. E., Flint, A. L., Flint, L. E., Gaye, C. B., Edmunds, W. M., and Ian, S.: Global synthesis of groundwater recharge in semi-arid and arid regions, *Hydrological Processes*, 20, 3335–3370, <https://doi.org/10.1002/hyp.6335>, 2006.
- Scanlon, B. R., Faunt, C. C., Longuevergne, L., Reedy, R. C., Alley, W. M., McGuire, V. L., and McMahon, P. B.: Groundwater depletion and sustainability of irrigation in the US High Plains and Central Valley, *Proceedings of the National Academy of Sciences*, 109, 9320–9325, <https://doi.org/10.1073/pnas.1200311109>, 2012.
- 900 Schaller, M. F. and Fan, Y.: River basins as groundwater exporters and importers: Implications for water cycle and climate modeling, *Journal of Geophysical Research Atmospheres*, 114, <https://doi.org/10.1029/2008JD010636>, 2009.
- Schuite, J., Longuevergne, L., Bour, O., Burbey, T. J., Boudin, F., Lavenant, N., and Davy, P.: Understanding the Hydromechanical Behavior of a Fault Zone From Transient Surface Tilt and Fluid Pressure Observations at Hourly Time Scales, *Water Resources Research*, 53, 10 558–10 582, <https://doi.org/10.1002/2017WR020588>, 2017.
- 905 Schuite, J., Flipo, N., Massei, N., Rivière, A., and Baratelli, F.: Improving the Spectral Analysis of Hydrological Signals to Efficiently Constrain Watershed Properties, *Water Resources Research*, 55, 4043–4065, <https://doi.org/10.1029/2018WR024579>, 2019.
- Shamsudduha, M., Taylor, R. G., Ahmed, K. M., and Zahid, A.: The impact of intensive groundwater abstraction on recharge to a shallow regional aquifer system: Evidence from Bangladesh, *Hydrogeology Journal*, 19, 901–916, <https://doi.org/10.1007/s10040-011-0723-4>, 2011.
- 910 Sililo, O. T. and Tellam, J. H.: Fingering in unsaturated zone flow: A qualitative review with laboratory experiments on heterogeneous systems, *Ground Water*, 38, 864–871, <https://doi.org/10.1111/j.1745-6584.2000.tb00685.x>, 2000.
- Simunek, J., Van Genuchten, M. T., and Sejna, M.: The HYDRUS-1D software package for simulating the one-dimensional movement of water, heat, and multiple solutes in variably-saturated media, *University of California-Riverside Research Reports*, 3, 1–240, 2005.
- Singhal, B. B. and Gupta, R. P.: *Applied hydrogeology of fractured rocks: Second edition*, Springer Science & Business Media, <https://doi.org/10.1007/978-90-481-8799-7>, 2010.
- 915 Taylor, R. G., Todd, M. C., Kongola, L., Maurice, L., Nahozya, E., Sanga, H., and MacDonald, A. M.: Evidence of the dependence of groundwater resources on extreme rainfall in East Africa, *Nature Climate Change*, 3, 374–378, <https://doi.org/10.1038/nclimate1731>, 2012.
- Taylor, R. G., Scanlon, B., Doell, P., Rodell, M., van Beek, R., Wada, Y., Longuevergne, L., Leblanc, M., Famiglietti, J. S., Edmunds, M., Konikow, L., Green, T. R., Chen, J., Taniguchi, M., Bierkens, M. F. P., MacDonald, A., Fan, Y., Maxwell, R. M., Yeichieli, Y., Gurdak, J. J., Allen, D. M., Shamsudduha, M., Hiscock, K., Yeh, P. J. F., Holman, I., and Treidel, H.: Ground water and climate change, *Nature Climate Change*, 3, 322–329, <https://doi.org/10.1038/nclimate1744>, 2013.
- 920 Thornthwaite, C. W.: An approach toward a rational classification of climate, *Geographical Review*, 38, 55–94, 1948.



- 925 Touchard, F.: Caractérisation hydrogéologique d'un aquifère en socle fracturé: Site de Ploemeur (Morbihan), <http://cat.inist.fr/?aModele=afficheN&cpsidt=193856>, 1999.
- Townley, L. R.: The response of aquifers to periodic forcing, *Advances in Water Resources*, 18, 125–146, [https://doi.org/10.1016/0309-1708\(95\)00008-7](https://doi.org/10.1016/0309-1708(95)00008-7), 1995.
- Troch, P. A., Martinez, G. F., Pauwels, V. R. N., Durcik, M., Sivapalan, M., Harman, C., Brooks, P. D., Gupta, H., and Huxman, T.: Climate and vegetation water use efficiency at catchment scales, <https://doi.org/10.1002/hyp.7358>, 2009.
- 930 Vergnes, J. P., Decharme, B., and Habets, F.: Introduction of groundwater capillary rises using subgrid spatial variability of topography into the ISBA land surface model, *Journal of Geophysical Research*, 119, 065–11, <https://doi.org/10.1002/2014JD021573>, 2014.
- Wada, Y., Van Beek, L. P. H., Van Kempen, C. M., Reckman, J. W. T. M., Vasak, S., and Bierkens, M. F. P.: Global depletion of groundwater resources, *Geophysical Research Letters*, 37, 1–5, <https://doi.org/10.1029/2010GL044571>, 2010.
- Wada, Y., Flörke, M., Hanasaki, N., Eisner, S., Fischer, G., Tramberend, S., Satoh, Y., Van Vliet, M. T., Yillia, P., Ringler, C., Burek, P.,  
935 and Wiberg, D.: Modeling global water use for the 21st century: The Water Futures and Solutions (WFaS) initiative and its approaches, *Geoscientific Model Development*, 9, 175–222, <https://doi.org/10.5194/gmd-9-175-2016>, 2016.
- Wright, E. P. and Burgess, W. G.: *The hydrogeology of crystalline basement aquifers in Africa*, Geological Society, London, Special Publications, 1992.
- Wyns, R., Baltassat, J. M., Lachassagne, P., Legchenko, A., Vairon, J., and Mathieu, F.: Application of proton magnetic resonance soundings  
940 to groundwater reserve mapping in weathered basement rocks (Brittany, France), *Bulletin de la Société Géologique de France*, 175, 21–34, <https://doi.org/10.2113/175.1.21>, 2004.